IEEE Access
Multidisciplinary | Rapid Review | Open Access Journal

SPECIAL SECTION ON PHYSICAL AND MEDIUM ACCESS CONTROL LAYER ADVANCES IN 5G WIRELESS NETWORKS

Received January 23, 2017; accepted February 22, 2017, date of publication April 5, 2017, date of current version June 7, 2017.

Digital Object Identifier 10.1109/ACCESS.2017.2690966

Stochastic Geometry-Based Modeling and Analysis of Citizens Broadband Radio Service System

PRIYABRATA PARIDA[1], (Student Member, IEEE), HARPREET S. DHILLON[1], (Member, IEEE), AND PAVAN NUGGEHALLI[2], (Member, IEEE)

[1]Wireless@VT, Department of ECE, Virginia Tech, Blacksburg, VA, USA
[2]MediaTek USA Inc., San Jose, CA, USA

Corresponding author: Priyabrata Parida (pparida@vt.edu)

This work was supported in part by the U.S. National Science Foundation under Grant CNS-1617896. The publication charges of this article were covered in part by Virginia Tech's Open Access Subvention Fund.

ABSTRACT In this paper, we model and analyze a cellular network that operates in the licensed band of the 3.5-GHz spectrum and consists of a licensed and an unlicensed operator. Using tools from stochastic geometry, we concretely characterize the performance of this spectrum sharing system. We model the locations of the licensed base stations (BSs) as a homogeneous Poisson point process with protection zones (PZs) around each BS. Since the unlicensed BSs cannot operate within the PZs, their locations are modeled as a Poisson hole process. In addition, we consider carrier sense multiple access with collision avoidance-type contention-based channel access mechanism for the unlicensed BSs. For this setup, we first derive an approximate expression and useful lower bounds for the medium access probability of the serving unlicensed operator BS. Furthermore, by efficiently handling the correlation in the interference powers induced due to correlation in the locations of the licensed and unlicensed BSs, we provide approximate expressions for the coverage probability of a typical user of each operator. Subsequently, we study the effect of different system parameters on area spectral efficiency of the network. To the best of our knowledge, this is the first attempt toward accurate modeling and analysis of a citizens broadband radio service system using tools from stochastic geometry.

INDEX TERMS Stochastic geometry, CBRS spectrum, Poisson hole process, medium access probability, coverage probability.

I. INTRODUCTION

Owing to the increasing usage of handheld devices, popularity of video steaming-based applications, and demand for ubiquitous connectivity, the mobile data traffic has been doubling every year for several years and the trend is expected to continue for the foreseeable future [2]. One obvious way of handling this data deluge is to make more spectrum available for the future generation (5G) of cellular networks. Although inclusion of millimeter wave frequencies (30 GHz – 300 GHz) in the cellular spectrum is expected to address this problem in a few years, a meaningful short-term solution is to use underutilized sub-6 GHz spectrum for cellular communication. One such example is the recent proposal by the Federal Communications Commission (FCC) to foster co-existence of commercial cellular networks alongside the defense communication systems [3] in the 3.5 GHz band, a.k.a. citizens broadband radio service (CBRS) band. As implied above already, one of the main advantages of the CBRS band is the mature hardware technology in the sub-6 GHz spectrum, which is suitable for near-future system deployment. For successful co-existence, the CBRS ecosystem is divided into three-tiered access systems: (1) incumbent access (IA) tier that consists of defense systems, (2) priority access licensed (PAL) tier for the licensed networks, and (3) general authorized access (GAA) tier for the unlicensed networks. Under key guidelines mentioned in [3], recent studies have shown that the co-existence between IA tier and PAL tier can be successfully achieved without violating the security and interference protection constraints of the defense systems while achieving appreciable data rates for the licensed communication networks [4]–[6]. However, from the commercial application perspective, the study on

successful co-existence of PAL and GAA networks (operators) is of prime importance, which has not been addressed in the literature and is the main focus of this work.

A. MOTIVATION AND RELATED WORKS

One of the key elements of the FCC guidelines is that the communication links of the licensed operator are to be protected from unlicensed BSs' interference by creating protection zones (PZs) around each licensed BS. Within these PZs, none of the unlicensed BSs are allowed to operate. The overall system is controlled by a centralized node known as the spectrum access system (SAS). While it is possible to centrally manage network operations such as spectrum access and transmission power control for the unlicensed BSs, doing so may result in increased signaling overhead due to potentially large number of unlicensed BSs. Hence, a preferable option is to perform some of the tasks, such as contention-based channel access among the unlicensed BSs, in a distributed manner. Consideration of contention-based channel access is also important since wireless LAN systems are likely to co-exist in this band. While one can, in principle, study the performance of this system through extensive simulations, simulators do not usually scale well with the growing number of nodes. As a result, it is highly desirable to develop a tractable approach capable of exposing fundamental performance trends of such large-scale systems.

One such approach that has received significant attention over the past few years is to contain the dimensionality of the problem by endowing the node locations with a distribution rather than assuming them to be deterministic. This allows one to conveniently compute network-wide metrics by spatially averaging over all possible topologies using powerful tools from stochastic geometry. This idea has already been applied successfully to analyze both cellular and ad hoc networks. Interested readers can refer to [7]–[13] for a pedagogical treatment of this research area. While it is natural to think that these existing tools and techniques may be directly applicable to the analysis of the CBRS system, it is not quite true. In particular, there are two CBRS-specific challenges that need to be overcome first: (1) the presence of PZs around licensed BSs creates correlation among the locations of licensed and unlicensed BSs that ultimately results in correlation among aggregate interference powers generated by the both sets of BSs; (2) presence of PZs, as well as the consideration of contention-based channel access mechanism, makes the statistical characterization of interference from unlicensed BSs a difficult task.

To the best of our knowledge, there exists no work in the literature that studies co-existence of licensed and unlicensed networks considering both PZs around licensed BSs and contention-based channel access mechanism among unlicensed BSs from the perspective of stochastic geometry. However, the performance of wireless systems considering either one of the above-mentioned key elements can be found in the literature. The performance of IEEE 802.11 network that considers carrier sense multiple access with collision avoidance (CSMA-CA) based contention access mechanism is presented in [14]. In the above work, the active node locations are modeled as a Matérn hardcore process of type-II (MHPP-II), and the performance analysis is presented in terms of the medium access probability (MAP) and the signal to interference ratio (SIR) coverage probability. The extension of the above approach to the performance analysis of cellular networks can be found in [15]. From the perspective of co-existence between licensed and unlicensed networks, in [16] and [17], MHPP-II is used to model contention-based channel access mechanism among primary and secondary transmitters. However, the performance analysis is limited to a bipolar ad hoc network. The extension of the above approach to a cellular setup for co-existence study between LTE and Wi-Fi systems is presented in [18]. However, in these works, the key system consideration regarding the node locations is in contrast to the FCC proposed model, where the spatial separation between licensed and unlicensed BSs is strictly enforced through PZs.

On the other hand, in order to capture the strict spatial separation among primary (licensed) and secondary (unlicensed) transmitters (BSs), in [19] authors have introduced Poisson hole process (PHP) and presented the performance analysis for a cognitive ad hoc network. However, in the system model, the distance between a transmitter and receiver pair is considered to be fixed, and contention-based channel access among secondary transmitters is not considered, which can degrade their performance considerably. To overcome the later limitation of [19], in [20] performance analysis of a cognitive network is presented considering Aloha protocol for channel access for the secondary transmitters, and in [21] considering exclusions zones around secondary transmitters so that two nearby secondary transmitters can not access the channel simultaneously. The extension of [19] to the performance analysis of heterogeneous cellular can be found in [22]. However, in all the above-mentioned works, the presence of holes (PZs) in the network is usually modeled by either thinning the unlicensed (secondary) transmitter density or by approximating the PHP with a cluster process. As a result, these approaches do not accurately model the correlation among the node locations. A more refined approach to the performance analysis of a PHP network in terms of coverage probability is presented in [23]. In particular, authors have provided useful bounds for the Laplace transform (LT) of interference that help in accurate coverage probability evaluation of a PHP network.

Unlike the prior art, where the effect of one of the two aspects of the FCC proposed system model is handled in isolation, we propose a unified analytic approach that takes into account the joint effect of both PZs and contention mechanisms. As we will see in following sections, this *joint* analysis is significantly challenging and requires a careful handling of several types of dependencies in the interference field to obtain accurate results for different performance metrics. Therefore, in addition to the contributions summarized

below, one indirect consequence of our analysis is the detailed exposition of several key open problems that appear in the performance analysis of a CBRS system.

B. CONTRIBUTIONS

1) SYSTEM MODELING

We propose a stochastic geometry-based framework to analyze the performance of a network that operates in the licensed band of the CBRS spectrum and consists of a licensed and an unlicensed operator. To be specific, we model the locations of the licensed BSs as a PPP and the locations of the unlicensed BSs as a PHP that takes into account the PZs around each licensed BS. In addition, a CSMA-CA type contention-based mechanism is also considered for medium access by the unlicensed BSs. This model captures the essential elements of the FCC envisioned system, whose key goal is to facilitate the symbiotic co-existence of the licensed and unlicensed operators.

2) SYSTEM ANALYSIS

For the system analysis of the licensed operator, the performance metrics that we consider are the SIR and the link rate coverage probability, as well as area spectral efficiency (ASE). Since ASE of the unlicensed operator depends on the MAP of its BSs, we derive an approximate expression and useful lower bounds for the MAP. Further, exact evaluation of coverage probabilities is difficult due to correlation in interference induced by the dependency in the licensed and unlicensed BS locations, as well as the presence of PZs. Hence, we provide approximate but fairly accurate results for coverage probabilities by carefully capturing the interference correlation and the effect of PZs in the vicinity of the typical user. In the process of evaluating the MAP and the coverage probability, we also provide approximate expressions for two useful distance distributions specific to the PHP network.

3) SYSTEM DESIGN INSIGHTS

Using the expressions for the MAP and the coverage probabilities, we study the impact of PZ radius and unlicensed BS transmission power on the network performance in terms of ASE. One important observation is that there exists an optimal operating point that maximizes the ASEs of the unlicensed operator and the overall network with respect to unlicensed BS transmission power. Another important observation is that the ASE of the unlicensed operator saturates beyond a certain carrier sense threshold.

II. SYSTEM MODEL

A. NETWORK GEOMETRY

We consider the downlink (DL) of a cellular network that has two operators, namely Operator A (OpA) and Operator B (OpB), operating in the licensed band of the CBRS spectrum. This band of the spectrum is divided into multiple frequency bands (FBs) of smaller bandwidth. Without loss of generality, we present our analysis for an arbitrarily selected FB (from amongst the smaller frequency bands) that we call the *representative FB*. We assume that OpA has the license to operate in PAL mode of operation, while OpB, as an unlicensed operator, can only operate in GAA mode of operation. Each operator is assumed to have deployed a set of citizens broadband service devices (CBSDs) (referred as BSs hereafter) in the region of consideration. The locations of the OpA BSs follow a homogeneous PPP Ψ_A of density λ_A. As per the FCC regulations, interference protection is provided to each OpA BS by considering a PZ around it, where operation of OpB BSs is prohibited. One reasonable way of modeling these interference protection zones is to assume that the OpB BSs form a PHP with the hole centers being the locations of the OpA BSs. In this case, the locations of OpB BSs in the PHP Φ_B are obtained by considering a baseline PPP Ψ_B of intensity λ_B and retaining only those points in Ψ_B that lie outside all the PZs, i.e.

$$\Phi_B = \left\{ \mathbf{x} \in \Psi_B : \prod_{\mathbf{y} \in \Psi_A} \mathbf{1}\left(\|\mathbf{y} - \mathbf{x}\| > R_{pz}\right) = 1 \right\}, \quad (1)$$

and the density of OpB BSs in Φ_B is given as

$$\hat{\lambda}_B = \lambda_B \exp(-\pi \lambda_A R_{pz}^2). \quad (2)$$

Above density follows from the null probability of PPP applied to Ψ_A that stems from the fact that for a typical point $\mathbf{x} \in \Psi_B$ to be in Φ_B, there should be no OpA BS within $\mathcal{B}_{R_{pz}}(\mathbf{x})$, i.e. a circle of radius R_{pz} centered at $\mathbf{x}$. Please refer [23, Lemma 2] for a formal proof.

We consider a closed-access system, where the OpA serves a set of *end users* (referred as users hereafter) whose locations form a homogeneous PPP ϑ_A and OpB serves another set of users whose locations form a homogeneous PPP ϑ_B. For simplicity, we assume that ϑ_A and ϑ_B are independent of each other as well as Ψ_A and Ψ_B. A user of an operator gets attached to its nearest BS belonging to that particular operator. In this work, we analyze the performance of a typical user of OpA (OpB) whose location is denoted by $\mathbf{u}_o^A$ ($\mathbf{u}_o^B$). Without loss of generality, we present the performance analysis considering $\mathbf{u}_o^A$ ($\mathbf{u}_o^B$) is placed at the origin. The serving BS of the typical user is termed as the *tagged* BS and its location is denoted as $\mathbf{x}_o^A$ ($\mathbf{x}_o^B$). In case of OpA, the distance $R_o^A = \|\mathbf{x}_o^A - \mathbf{u}_o^A\|$ between the typical user and the tagged BS follows Rayleigh distribution, which is given as

$$f_{R_o^A}(r_o^A) = 2\pi \lambda_A r_o^A \exp(-\pi \lambda_A (r_o^A)^2). \quad (3)$$

Above expression is the probability density function (PDF) of the contact distance for a homogeneous PPP [12]. On the other hand, for the OpB, the distribution of the distance $R_o^B = \|\mathbf{x}_o^B - \mathbf{u}_o^B\|$, between the typical user and the serving BS corresponds to the contact distance distribution for PHP. Accurate characterization of this distance distribution requires the consideration of the relative overlaps among the PZs, as well as the probability of the PZs deleting the points of Ψ_B in a given region. Owing to its analytical complexity, characterization of the contact distance distribution of PHP remains an open

TABLE 1. Summary of notations.

Notation	Description
Ψ_A, λ_A	Homogeneous PPP modeling the locations OpA BSs, density of Ψ_A
Φ_B	PHP modeling the locations of OpB BSs
Ψ_B, λ_B	Parent homogeneous PPP for Φ_B, density of Ψ_B
R_{pz}	Protection zone radius
$\mathbf{u}_o^A, \mathbf{u}_o^B$	Locations of the typical OpA and OpB users
$\mathbf{x}_o^A, \mathbf{x}_o^B$	Locations of the tagged OpA and OpB BSs
R_o^A	Distance between a typical user and its nearest OpA BS
R_o^B	Distance between the typical OpB user and tagged OpA BS
D_o^B	Distance between the typical OpA user and its nearest active OpB BS
$R_{o,AB}$	Distance between the tagged OpB BS and its nearest OpA BS
P_A, P_B	Transmission power per unit bandwidth of OpA and OpB BSs
$P_r(\mathbf{y}, \mathbf{x}_i)$	Received power per unit bandwidth at a location $\mathbf{y}$ from a location $\mathbf{x}_i$
$\mathcal{I}_o^B$	Medium access indicator of the tagged OpB BS
$\mathcal{M}_o^B$	Medium access probability of the tagged OpB BS
τ_{cs}	Carrier sense threshold
$\mathtt{SIR}_o^A, \mathtt{SIR}_o^B$	The SIR for the typical OpA and OpB user
$\mathtt{P}_\mathtt{C}^{(\mathtt{A})}(T)/\mathtt{P}_\mathtt{C}^{(\mathtt{B})}(T)$	Coverage probability of typical typical OpA/ OpB user for a target SIR threshold of T
$\mathcal{B}_r(\mathbf{x})$	A circle of radius r centered at $\mathbf{x}$.
$N_\Psi(\mathcal{C})$	Number of points of the point process Ψ that lie in the region $\mathcal{C}$
$\lvert\mathcal{C}\rvert$	The area of the region $\mathcal{C}$

problem. Having said that, in the literature, the PDF of R_o^B is approximated as Weibull distribution (cf. [22]) and is given as

$$f_{R_o^B}(r_o^B; \alpha, \beta) \approx \frac{\beta}{\alpha}\left(\frac{r_o^B}{\alpha}\right)^{\beta-1} \exp\left(-\frac{r_o^B}{\alpha}\right)^{\beta}, \tag{4}$$

where α is the shape parameter and β is the scale parameter of the function. Corresponding CDF is given as

$$F_{R_o^B}(r_o^B; \alpha, \beta) \approx 1 - \exp\left(-\frac{r_o^B}{\alpha}\right)^{\beta}. \tag{5}$$

The values of these parameters depend on λ_A, λ_B, and R_{pz} and are determined through curve-fitting for a given set of system parameters.

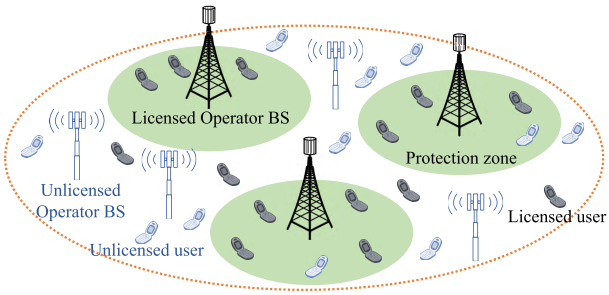

FIGURE 1. As illustration of the CBRS network studied in this paper.

An illustration of the CBRS network studied in this paper is presented in Fig 1. Further, a representative network diagram where a typical user of OpA (OpB) is served by the tagged OpA (OpB) BS is presented in Fig. 2a (Fig. 2b). For quick reference, the notation used in this paper is summarized in Table 1.

B. PROPAGATION MODEL

The representative FB is divided into a certain number of orthogonal time-frequency resources known as resource blocks. We assume that the channel gain on each resource block is affected by path loss and multi-path fading. Multi-path fading is assumed to be Rayleigh distributed and independent across resource blocks. For simplicity, we ignore the effect of shadowing. Without loss of generality, we present our analysis for a *representative resource block*. The transmission power spectral density, i.e. transmission power per unit bandwidth of OpA (OpB) is P_A (P_B). Now, on the representative resource block, the received power per unit bandwidth at a generic location $\mathbf{y}$ from a BS located at $\mathbf{x}_i \in \Psi_A$ or Φ_B is given as

$$P_r(\mathbf{y}, \mathbf{x}_i) = \frac{P_T h(\mathbf{y}, \mathbf{x}_i)}{l(\|\mathbf{y} - \mathbf{x}_i\|)}, \tag{6}$$

where P_T can be P_A or P_B, $l(\|\mathbf{y} - \mathbf{x}_i\|)$ is the path loss in linear scale, and $h(\mathbf{y}, \mathbf{x}_i)$ is the multi-path gain of the channel between the BS at $\mathbf{x}_i$ and the receiver node at $\mathbf{y}$. We assume that the multi-path fading gains are i.i.d. among links between different nodes. Since the amplitude of multi-path fading is assumed to be Rayleigh distributed, the multi-path gain $h(\mathbf{y}, \mathbf{x}_i) \sim \exp(1)$. In this work, we consider Urban Micro non-line-of-sight path loss model [24], which is characterized as

$$10\log_{10}(l(d)) = 36.7\log_{10}(d) + 22.7 + 26\log_{10}(f_c), \tag{7}$$

where d is the distance between the two nodes in meters and $f_c = 3.5$ GHz is the carrier frequency.

C. CONTENTION-BASED MEDIUM ACCESS MECHANISM

For successful co-existence of OpB BSs in GAA mode of operation, a contention-based channel access mechanism is necessary. In this work, we consider CSMA-CA based channel access mechanism that is prevalent in Wireless LAN (WLAN) systems. This access mechanism is divided into two phases, namely *listen before talk* (LBT) and *contention*. In the LBT phase, a potential BS tries to detect

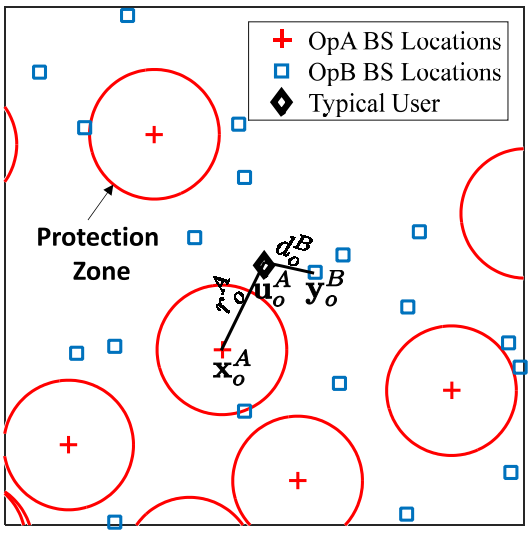

(a)

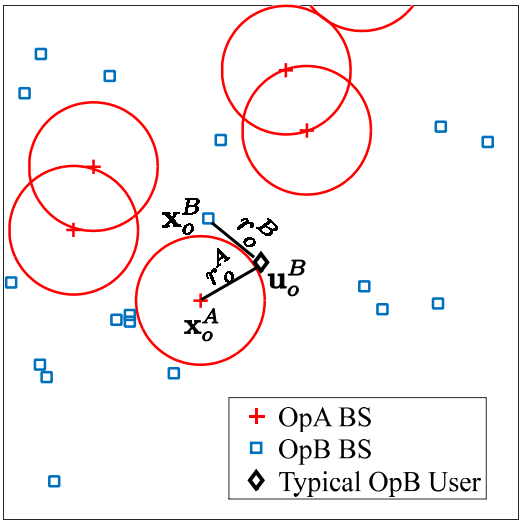

(b)

FIGURE 2. (a) Typical OpA user located at $\mathbf{u}_o^A$ served by the tagged OpA BS at $\mathbf{x}_o^A$. (b) Typical OpB user located at $\mathbf{u}_o^B$ is served by the tagged OpB BS located at $\mathbf{x}_o^B$.

the presence of other active BSs, where the detection is successful if the potential BS is able to decode one of the received preambles from active BSs. Successful decoding of a preamble requires the received signal strength to be above certain threshold known as carrier sense threshold (τ_{cs}). If the received signal strength is more than the carrier sense threshold, the potential BS waits till the end of the transmission followed by contention phase. In contention phase, the potential BS does a random back-off, where the back-off timer depends on the contention window size, which is a system implementation parameter. On the other hand, if the potential BS observes the channel to be idle during LBT phase (i.e. received signal strength from each of the active BSs is less than τ_{cs}), then it reduces its back-off timer. This process

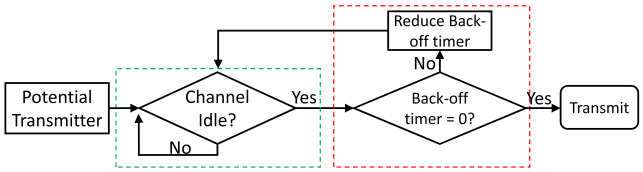

FIGURE 3. A simplified flow chart of CSMA-CA. The green dotted rectangle corresponds to the LBT phase and the red dotted rectangle corresponds to the contention phase.

continues until the back-off timer is zero after which the BS transmits its data immediately. In case the back-off timers of two BSs are the same, advanced protocols are used to avoid the packet collision. A flow chart of the above procedure is presented in Fig. 3.

Based on the above-mentioned channel access mechanism, to model the *active* OpB BSs that access the channel simultaneously, we follow the same formulation as presented in [14]. We briefly describe this for the tagged OpB BS located at $\mathbf{x}_o^B \in \Phi_B$. The tagged BS wins contention w.r.t. a BS at $\mathbf{x}_j^B$ if either of the following events takes place:

1. The received signal strength from a BS at $\mathbf{x}_j^B$ is less than τ_{cs}, i.e. the BS at $\mathbf{x}_j^B$ does not lie in the *contention domain* of the BS at $\mathbf{x}_o^B$.

2. The received signal strength from the BS at $\mathbf{x}_j^B$ is more than the threshold τ_{cs}, but its back-off timer $t_{x_j^B}$ is larger than the back-off timer $t_{x_o^B}$ of the tagged BS. Similar to [14], we assume that the back-off timers are uniformly distributed between [0, 1].

Now if the BS at $\mathbf{x}_o^B$ wins contention w.r.t. all other BSs in Φ_B, then it gets access to the channel. Based on the above discussion, the medium access indicator of the BS $\mathbf{x}_o^B$ is given as $\mathcal{I}_o^B =$

$$\prod_{\mathbf{x}_j^B \in \Phi_B \setminus \mathbf{x}_o^B} \left(\mathbf{1}_{P_r(\mathbf{x}_o^B, \mathbf{x}_j^B) \le \tau_{cs}} + \mathbf{1}_{P_r(\mathbf{x}_o^B, \mathbf{x}_j^B) > \tau_{cs}} \mathbf{1}_{t_{x_j^B} > t_{x_o^B}} \right). \tag{8}$$

where $P_r(\cdot, \cdot)$ is defined in (6). Now, the MAP of the tagged OpB BS is given as $\mathcal{M}_o^B = \mathbb{P}\left[\mathcal{I}_o^B = 1\right] =$

$$\mathbb{E}\left[\prod_{\mathbf{x}_j^B \in \Phi_B \setminus \mathbf{x}_o^B} \left(\mathbf{1}_{P_r(\mathbf{x}_o^B, \mathbf{x}_j^B) \le \tau_{cs}} + \mathbf{1}_{P_r(\mathbf{x}_o^B, \mathbf{x}_j^B) > \tau_{cs}} \mathbf{1}_{t_{x_j^B} > t_{x_o^B}} \right) \right]. \tag{9}$$

D. PERFORMANCE METRICS

We evaluate the performance of OpA and OpB networks, using the following metrics:

1) COVERAGE PROBABILITY

Under the assumption of an interference limited network, the SIR of a typical OpB user is defined as

$$\mathtt{SIR}_o^B = \frac{\mathcal{I}_o^B P_r(\mathbf{u}_o^B, \mathbf{x}_o^B)}{I_{agg}^{BB} + I_{agg}^{BA}}, \tag{10}$$

where $I_{agg}^{BB} = \sum_{\mathbf{x}_j^B \in \Phi_B \setminus \mathbf{x}_o^B} \mathcal{I}_j^B P_r(\mathbf{u}_o^B, \mathbf{x}_j^B)$, and $I_{agg}^{BA} = \sum_{\mathbf{y}_j^A \in \Psi_A} P_r(\mathbf{u}_o^B, \mathbf{y}_j^A)$ are the aggregate interference powers received at the typical OpB user from the OpB and OpA BSs, respectively. Now, the SIR coverage probability is defined as the probability that the SIR at the typical user is greater than a target threshold T. In this work, we present the SIR coverage probability for the typical OpB user when the tagged BS is active, i.e. $\mathcal{I}_o^B = 1$. Hence, for a target SIR threshold T, this is formally expressed as

$$\mathtt{P}_{\mathtt{C}}^{(\mathtt{B})}(T) = \mathbb{P}\Big[\mathtt{SIR}_o^B > T | \mathcal{I}_o^B = 1\Big]. \tag{11}$$

Similarly, the link rate coverage probability of the typical OpB user for a target threshold T is defined as

$$\begin{aligned}\mathtt{R}_{\mathtt{C}}^{(\mathtt{B})}(T) &= \mathbb{P}\Big[B_w \log_2(1+\mathtt{SIR}_o^B) > T | \mathcal{I}_o^B = 1\Big] \\ &= \mathbb{P}\Big[\mathtt{SIR}_o^B > 2^{T/B_w} - 1 | \mathcal{I}_o^B = 1\Big],\end{aligned} \tag{12}$$

where B_w denotes bandwidth.

On the other hand, for the typical OpA user, the coverage probability can be expressed as

$$\mathtt{P}_{\mathtt{C}}^{(\mathtt{A})}(T) = \mathbb{P}\Big[\mathtt{SIR}_o^A > T\Big] = \mathbb{P}\Big[\frac{P_r(\mathbf{u}_o^A, \mathbf{x}_o^A)}{I_{agg}^{AB} + I_{agg}^{AA}} > T\Big], \tag{13}$$

where $I_{agg}^{AB} = \sum_{\mathbf{x}_j^B \in \Phi_B} \mathcal{I}_j^B P_r(\mathbf{u}_o^A, \mathbf{x}_j^B)$ is the interference received at the typical OpA user from OpB BSs, and $I_{agg}^{AA} = \sum_{\mathbf{x}_j^A \in \Psi_A \setminus \mathbf{x}_o^A} P_r(\mathbf{u}_o^A, \mathbf{x}_j^A)$ is the interference received from OpA BSs. Similar to the previous case, for a target threshold T, the link rate coverage probability for the typical OpA user is defined as

$$\begin{aligned}\mathtt{R}_{\mathtt{C}}^{(\mathtt{A})}(T) &= \mathbb{P}\Big[B_w \log_2(1+\mathtt{SIR}_o^A) > T\Big] \\ &= \mathbb{P}\Big[\mathtt{SIR}_o^A > 2^{T/B_w} - 1\Big].\end{aligned} \tag{14}$$

2) AREA SPECTRAL EFFICIENCY (ASE):

In this paper, we define the ASE of the network for a target SIR threshold T as

$$\mathcal{A}(T) = \Big(\hat{\lambda}_B \mathcal{M}_o^B \mathtt{P}_{\mathtt{C}}^{(\mathtt{B})}(T) + \lambda_A \mathtt{P}_{\mathtt{C}}^{(\mathtt{A})}(T)\Big) \log_2(1+T). \tag{15}$$

Note that it is more precise to use the coverage probabilities and MAP computed from the typical BS perspective in the above expression. However, in order to maintain tractability, we use the ones computed for the tagged BS (equivalently the typical user), which provides a reasonable approximation. While there is a subtle difference in the two viewpoints, either is sufficient to expose macroscopic system-level trends, which is the main purpose of our analysis.

From the definition of performance metrics it is clear that theoretical expressions for following metrics are necessary: (1) MAP of the tagged OpB BSs, and (2) SIR coverage probability of a typical OpA (OpB) user. In the next section, we characterize these quantities.

III. MEDIUM ACCESS PROBABILITY FOR THE TAGGED OPB BS

Before deriving the main results, we present the following Lemma that is going to be useful in the derivation of several relevant distance distributions and conditional density functions of Ψ_A and Φ_B in the subsequent sections.

Lemma 1 (Presence of a hole in a homogeneous PPP): Consider a homogeneous PPP Ψ of density λ and a hole of radius R located at an arbitrary point $\mathbf{y} \in \mathbb{R}^2$. Conditioned on the distance $\|\mathbf{y}\|$ between the hole center and the origin, the intensity measure of Ψ is given as $\Lambda_\Psi(\mathcal{B}_x(\mathbf{o}) | \|\mathbf{y}\|) = \mathcal{G}(x, \lambda, R, \|\mathbf{y}\|) =$

$$\begin{cases} 0 & \|\mathbf{y}\| \le R, 0 \le x \le R - \|\mathbf{y}\| \\ \pi\lambda x^2 & \|\mathbf{y}\| > R, 0 \le x \le \|\mathbf{y}\| - R \\ \lambda(\pi x^2 - A(x, R, \|\mathbf{y}\|)) & |\|\mathbf{y}\| - R| < x \le \|\mathbf{y}\| + R \\ \pi\lambda x^2 - \pi\lambda R^2 & x > \|\mathbf{y}\| + R, \end{cases} \tag{16}$$

where $\mathbf{o} = (0,0)$ *is the origin, and* $A(r, R, d) =$

$$\begin{aligned} &r^2 \cos^{-1}\left(\frac{r^2 + d^2 - R^2}{2rd}\right) + R^2 \cos^{-1}\left(\frac{R^2 + d^2 - r^2}{2Rd}\right) \\ &\quad - \frac{1}{2}\sqrt{(r + R - d)(r + R + d)(d + r - R)(d - r + R)}, \end{aligned} \tag{17}$$

which represents the area of intersection of two circles with radii r and R, and their centers are separated by a distance d. Corresponding conditional density function is given as

$$\lambda_\Psi(x | \|\mathbf{y}\|) = \frac{1}{2\pi x} \frac{\mathrm{d}\Lambda_\Psi(\mathcal{B}_x(\mathbf{o}) | \|\mathbf{y}\|)}{\mathrm{d}x} \equiv \mathcal{E}(x, \lambda, R, \|\mathbf{y}\|). \tag{18}$$

The derivative of $A(r, R, d)$ with respect to r is given in (19) *at the bottom of the next page.*

Proof: The intensity measure of a point process is defined as the average number of points that lie within a given area [10]. In this case, we are interested in finding the average number of points of Ψ that lie in $\mathcal{B}_x(\mathbf{o}) \setminus \{\mathcal{B}_x(\mathbf{o}) \cap \mathcal{B}_R(\mathbf{y})\}$. Depending on the location of the hole from the origin, the average number of points that lie in $\mathcal{B}_x(\mathbf{o}) \cap \mathcal{B}_R(\mathbf{y})$ would be different, which is captured in (16). Fig. 4a represents the third case of (16). The other cases of interest involve either complete overlap or no overlap between the circles $\mathcal{B}_x(\mathbf{o})$ and $\mathcal{B}_R(\mathbf{y})$, and illustrations are omitted to avoid repetition. ■

A. MAP OF THE TAGGED OpB BS

In this section, we present the MAP of the tagged OpB BS, which is an important intermediate metric as it is useful in obtaining the ASE of the OpB network. In (9), MAP is expressed as the product of the indicator functions that represent the contention winning event of the tagged BS w.r.t. the

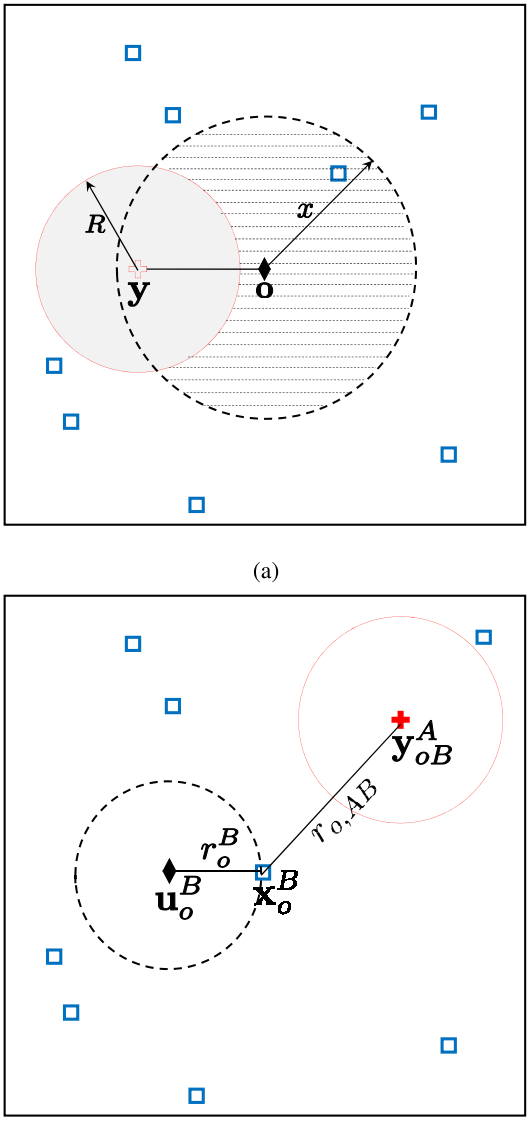

FIGURE 4. (a) Illustration of a PPP with a hole for Lemma 1. The blue squares represent the set of points in Ψ. The red cross is the center of a hole with radius R. (b) A representative network diagram for Lemma 2.

rest of the BSs in Φ_B. In point process theory, this product is evaluated using probability generating functional (PGFL) of the underlying point process [10, Ch. 4]. However, the PGFL for a PHP is not known [19], and any attempt to characterizing it involves exact consideration of relative overlaps among PZs, which is not straightforward. The approach that is usually followed in the literature to circumvent this problem is to approximate the PHP by a PPP. The density of the approximated PPP is either set to the density of baseline PPP Ψ_B (by completely ignoring the PZs) or to $\hat{\lambda}_B$ defined in (2) (cf. [19]). However, it has been shown recently in [23] that the interference field of a PHP can be accurately bounded by simply considering the exact effect of the closest hole while ignoring the rest of the holes. In the context of our work, this means that we can bound Φ_B with the baseline process Ψ_B from where the points lying in the PZ nearest to the tagged BS are removed. Clearly, the consideration of only the nearest PZ gives a lower bound on the MAP as more number of points are taken into consideration for the contention process than the actual number of BSs in Φ_B.

1) CONDITIONAL MAP OF THE TAGGED OpB BS

In this subsection, we derive a lower bound on the MAP of the tagged BS conditioned on its distance from the typical user and the nearest OpA BS, which is the center of its nearest PZ.

Lemma 2: The MAP *of the tagged OpB BS at* $\mathbf{x}^B_o \in \Phi_B$ *conditioned on its distances* $R_{o,AB}$ *from the nearest OpA BS and* R^B_o *from the typical user is given as*

$$\mathbb{P}\left[\mathcal{I}^B_o = 1 \middle| r_{o,AB}, r^B_o\right] \geq \frac{1-\exp(-f_1(r_{o,AB}, r^B_o))}{f_1(r_{o,AB}, r^B_o)}, \tag{20}$$

where $f_1(r_{o,AB}, r^B_o) =$

$$2\Big(\pi \int_0^{\infty} \lambda_{\Psi_B}(y|r^B_o) e^{\frac{-\tau_{CS} l(y)}{P_B}} y \mathrm{d}y - \int_{r_{o,AB}-R_{pz}}^{r_{o,AB}+R_{pz}} \lambda_{\Psi_B}(y|r^B_o) e^{\frac{-\tau_{CS} l(y)}{P_B}} \varphi_{pz}(y|r_{o,AB}) y \mathrm{d}y\Big), \tag{21}$$

$\varphi_{pz}(y|x) = \arccos\left(\frac{y^2+x^2-R^2_{pz}}{2xy}\right)$, *and* $\lambda_{\Psi_B}(y|r^B_o) = \mathcal{E}(y, \lambda_B, r^B_o, r^B_o)$ *as given in* (18).

Proof: Please refer to Appendix A. ■

In order to obtain the final expression for MAP, we need to decondition the conditional MAP result derived above w.r.t. the distributions of R^B_o and $R_{o,AB}$. While R^B_o is approximated to follow Weibull distribution and given in (4), the distance distribution for $R_{o,AB}$ is not known. Further, as we discuss

$$\begin{aligned}\frac{\mathrm{d}A(r,R,d)}{\mathrm{d}r} = &-\frac{r^2\left(\frac{1}{d}-\frac{r^2+d^2-R^2}{2r^2d}\right)}{\sqrt{1-\frac{(r^2+d^2-R^2)^2}{4r^2d^2}}} + 2r\arccos\left(\frac{r^2+d^2-R^2}{2rd}\right) + \frac{Rr}{d\sqrt{1-\frac{(R^2-r^2+d^2)^2}{4R^2d^2}}} \\ &- \frac{(r+R-d)(R-r+d)(r-R+d)+(R+r-d)(R-r+d)(R+r+d)}{4\sqrt{(r+R-d)(r+R+d)(r-R+d)(R-r+d)}} \\ &+ \frac{(R+r-d)(-R+r+d)(R+r+d)-(R-r+d)(r-R+d)(R+r+d)}{4\sqrt{(r+R-d)(r+R+d)(r-R+d)(R-r+d)}}.\end{aligned} \tag{19}$$

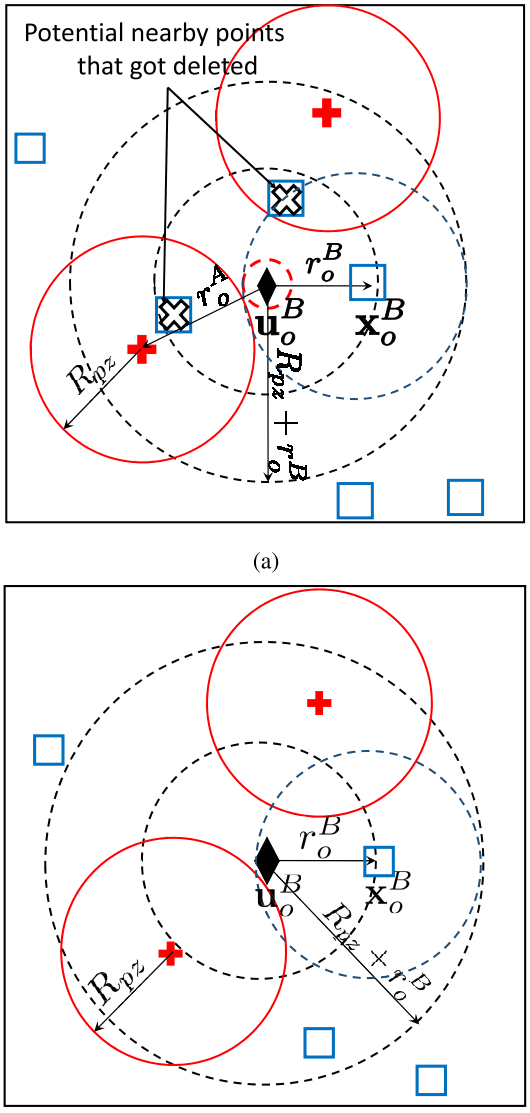

FIGURE 5. The diamond, crosses, and squares represent the locations of the typical OpB user, OpA BSs, and OpB BSs, respectively. The location of the typical user is $\mathbf{u}_o^B = (0, 0)$ and the tagged OpB BS is $\mathbf{x}_o^B = (r_o^B, 0)$. (a) An Illustration of Event-1. (b) An Illustration of Event-2.

later in this section, R_o^B and $R_{o,AB}$ are dependent random variables. Hence, the above deconditioning needs to be performed using the joint distribution of R_o^B and $R_{o,AB}$. In the following two subsections, we present an approximate expression and useful lower bounds for the CDF of $R_{o,AB}$ conditioned on R_o^B, as well as lower bound and approximate expressions for the MAP of the tagged BS considering the joint distribution of $R_{o,AB}$ and R_o^B.

2) LOWER BOUNDS AND APPROXIMATE EXPRESSION FOR CDF OF $R_{o,AB}$

Since the tagged BS is a point in the PHP Φ_B, there are no OpA BSs inside the circle $\mathcal{B}_{R_{pz}}(\mathbf{x}_o^B)$. Now, for a given realization of R_o^B (i.e. r_o^B) between the typical user and the tagged BS, the density of OpA BSs in the vicinity of the tagged BS beyond $\mathcal{B}_{R_{pz}}(\mathbf{x}_o^B)$ depends on the following two events:

- Event-1 (Illustrated in Fig. 5a): The tagged BS at $\mathbf{x}_o^B$ is not the nearest point to the typical user in the baseline PPP Ψ_B, i.e. points in Ψ_B closer to the typical user than $\mathbf{x}_o^B$ are deleted by the PZ(s). This event indicates that there is at least one OpA BS in $\mathcal{B}_{r_o^B+R_{pz}}(\mathbf{u}_o^B) \setminus \mathcal{B}_{R_{pz}}(\mathbf{x}_o^B)$ (hence in the vicinity of the tagged OpB BS) that has deleted the points in Ψ_B. Therefore, in this case, the density of OpA BSs in the vicinity of the typical user is likely to be higher than λ_A as the probability of having no OpA BS in $\mathcal{B}_{r_o^B+R_{pz}}(\mathbf{u}_o^B)$ is zero. Further, the higher density is also intuitively justified by the argument that to ensure all the points of Ψ_B in $\mathcal{B}_{r_o^B}(\mathbf{u}_o^B)$ are deleted, the density of OpA BSs in $\mathcal{B}_{r_o^B+R_{pz}}(\mathbf{u}_o^B) \setminus \mathcal{B}_{R_{pz}}(\mathbf{x}_o^B)$ is likely to be larger than λ_A.
- Event-2 (Illustrated in Fig. 5b): The location of the tagged BS $\mathbf{x}_o^B \in \Phi_B$ is the nearest point to the typical user in the baseline PPP Ψ_B. In this case, the locations of OpA BSs follow a homogeneous PPP of density λ_A beyond the circle $\mathcal{B}_{R_{pz}}(\mathbf{x}_o^B)$. Further, in contrast to Event-1, in this case, the knowledge of r_o^B does not convey any information regarding the distribution of $R_{o,AB}$. Hence, R_o^B is independent of $R_{o,AB}$.

Taking both the events into account, the CDF of $R_{o,AB}$ conditioned on the distance to the tagged BS R_o^B is given in (22) at the top of the next page. While the CDF of $R_{o,AB}$ conditioned on Event-1 and Event-2, can be obtained in different ways, in our case, we first condition on the distance R_o^A between the typical user to its nearest OpA BS and then obtain the CDF expression. Hence, (22) can be further expanded as

$$\begin{aligned}
&\mathbb{P}\Big[R_{o,AB} \le r_{o,AB} | r_o^B, N_{\Phi_B}(\mathcal{B}_{r_o^B}(\mathbf{u}_o^B)) = 0\Big] \\
&= \int_{r_o^A=0}^{\infty} \underbrace{\mathbb{P}\Big[R_{o,AB} \le r_{o,AB} | r_o^A, r_o^B, E_1(r_o^B)\Big]}_{K_1} \\
&\quad \times f_{R_o^A}(r_o^A | r_o^B, E_1(r_o^B)) \mathrm{d}r_o^A \\
&\mathbb{P}\Big[N_{\Psi_B}(\mathcal{B}_{r_o^B}(\mathbf{u}_o^B)) \ne 0 \Big| N_{\Phi_B}(\mathcal{B}_{r_o^B}(\mathbf{u}_o^B)) = 0, r_o^B\Big] \\
&\quad + \int_{r_o^A=0}^{\infty} \underbrace{\mathbb{P}\Big[R_{o,AB} \le r_{o,AB} | r_o^A, r_o^B, E_2(r_o^B)\Big]}_{K_2} \\
&\quad \times f_{R_o^A}(r_o^A | r_o^B, E_2(r_o^B)) \mathrm{d}r_o^A \\
&\mathbb{P}\Big[N_{\Psi_B}(\mathcal{B}_{r_o^B}(\mathbf{u}_o^B)) = 0 \Big| N_{\Phi_B}(\mathcal{B}_{r_o^B}(\mathbf{u}_o^B)) = 0, r_o^B\Big]. \qquad (23)
\end{aligned}$$

From the above expression it is clear that to obtain the CDF of $R_{o,AB}$ conditioned on R_o^B, we need to compute the expressions for K_1, K_2 and the PDF of R_o^A conditioned on Event-1 and Event-2. It is relatively simple to obtain the expression for K_2

$$
\begin{aligned}
&F_{R_{o,AB}}(r_{o,AB}|r_o^B)\\
&= \mathbb{P}\Big[R_{o,AB} \le r_{o,AB}|r_o^B, N_{\Phi_B}(\mathcal{B}_{r_o^B}(\mathbf{u}_o^B)) = 0\Big]\\
&= \mathbb{P}\Big[R_{o,AB} \le r_{o,AB}\Big|r_o^B, N_{\Phi_B}(\mathcal{B}_{r_o^B}(\mathbf{u}_o^B)) = 0, N_{\Psi_B}(\mathcal{B}_{r_o^B}(\mathbf{u}_o^B)) \ne 0\Big]\mathbb{P}\Big[N_{\Psi_B}(\mathcal{B}_{r_o^B}(\mathbf{u}_o^B)) \ne 0\Big|N_{\Phi_B}(\mathcal{B}_{r_o^B}(\mathbf{u}_o^B)) = 0, r_o^B\Big]\\
&\quad+\mathbb{P}\Big[R_{o,AB} \le r_{o,AB}\Big|r_o^B, N_{\Phi_B}(\mathcal{B}_{r_o^B}(\mathbf{u}_o^B)) = 0, N_{\Psi_B}(\mathcal{B}_{r_o^B}(\mathbf{u}_o^B)) = 0\Big]\mathbb{P}\Big[N_{\Psi_B}(\mathcal{B}_{r_o^B}(\mathbf{u}_o^B)) = 0\Big|N_{\Phi_B}(\mathcal{B}_{r_o^B}(\mathbf{u}_o^B)) = 0, r_o^B\Big]\\
&= \mathbb{P}\Big[R_{o,AB} \le r_{o,AB}\Big|r_o^B, E_1(r_o^B)\Big]\mathbb{P}\Big[N_{\Psi_B}(\mathcal{B}_{r_o^B}(\mathbf{u}_o^B)) \ne 0\Big|N_{\Phi_B}(\mathcal{B}_{r_o^B}(\mathbf{u}_o^B)) = 0, r_o^B\Big]\\
&\quad+\mathbb{P}\Big[R_{o,AB} \le r_{o,AB}\Big|r_o^B, E_2(r_o^B)\Big]\mathbb{P}\Big[N_{\Psi_B}(\mathcal{B}_{r_o^B}(\mathbf{u}_o^B)) = 0\Big|N_{\Phi_B}(\mathcal{B}_{r_o^B}(\mathbf{u}_o^B)) = 0, r_o^B\Big],
\end{aligned}
\tag{22}
$$

where $N_{\Phi_B}(\mathcal{B}_{r_o^B}(\mathbf{u}_o^B))$ and $N_{\Psi_B}(\mathcal{B}_{r_o^B}(\mathbf{u}_o^B))$ represent the number of points of Φ_B and Ψ_B in $\mathcal{B}_{r_o^B}(\mathbf{u}_o^B)$, respectively. Further, $E_1(r_o^B)$ represents $\{N_{\Phi_B}(\mathcal{B}_{r_o^B}(\mathbf{u}_o^B)) = 0, N_{\Psi_B}(\mathcal{B}_{r_o^B}(\mathbf{u}_o^B)) \ne 0\}$ and $E_2(r_o^B)$ represents $\{N_{\Phi_B}(\mathcal{B}_{r_o^B}(\mathbf{u}_o^B)) = 0, N_{\Psi_B}(\mathcal{B}_{r_o^B}(\mathbf{u}_o^B)) = 0\}$.

as Ψ_A is a homogeneous PPP of density λ_A beyond $\mathcal{B}_{R_{pz}}(\mathbf{x}_o^B)$. On the other hand, as explained earlier, the conditional CDF of $R_{o,AB}$ given by K_1 is not trivial to obtain as the conditional density of Ψ_A in $\mathcal{B}_{r_o^B+R_{pz}}(\mathbf{u}_o^B) \setminus \mathcal{B}_{R_{pz}}(\mathbf{x}_o^B)$ is difficult to characterize. Hence, for Event-1, we assume Ψ_A to follow homogeneous PPP of density λ_A in $\mathcal{B}_{r_o^B+R_{pz}}(\mathbf{u}_o^B) \setminus \mathcal{B}_{R_{pz}}(\mathbf{x}_o^B)$. In other words, we approximate K_1 by K_2. Therefore, we are now left with the task to obtain the expression for K_2. To do so, consider the following two events:

1) The nearest OpA BS to the typical user is also the nearest OpA BS for the tagged OpB BS. Let $\hat{R}_{o,AB}$ denotes the distance between the OpB tagged BS and the nearest OpA BS to the typical user. An illustration is provided in Fig. 6a. Note that the nearest OpA BS to the typical user is located at $\mathbf{x}_o^A$ and there are no BSs in the circle $\mathcal{B}_{\hat{R}_{o,AB}}(\mathbf{x}_o^B)$, where
$$\hat{R}_{o,AB} = \sqrt{(r_o^A)^2 + (r_o^B)^2 - 2r_o^A r_o^B \cos(\Theta_A)}, \tag{24}$$
where Θ_A is the angle between the lines joining the points $\mathbf{x}_o^B, \mathbf{u}_o^B$ and $\mathbf{x}_o^A, \mathbf{u}_o^B$ (refer to Fig. 6a for an illustration). Further, the randomness in $\hat{R}_{o,AB}$ is due to Θ_A.
2) The other event of interest is the scenario where the nearest PZ to the tagged BS is different from the nearest PZ to the typical user, i.e. there is at least one BS in $\mathcal{B}_{\hat{R}_{o,AB}}(\mathbf{x}_o^B)$ as illustrated Fig. 6b.

Taking into account both the events, we can write

$$R_{o,AB} = \begin{cases} \hat{R}_{o,AB} & N_{\Psi_A}\Big(\mathcal{C}_1(\hat{R}_{o,AB})\Big) = 0 \\ \tilde{R}_{o,AB} & N_{\Psi_A}\Big(\mathcal{C}_1(\hat{R}_{o,AB})\Big) \ne 0, \end{cases} \tag{25}$$

where

$$\mathcal{C}_1(x) = \mathcal{B}_x(\mathbf{x}_o^B) \setminus \left\{\mathcal{B}_{r_o^A}(\mathbf{u}_o^B) \cup \mathcal{B}_{R_{pz}}(\mathbf{x}_o^B)\right\}, \tag{26}$$

$\tilde{R}_{o,AB}$ is the distance to the nearest OpA BS that lies in $\mathcal{C}_1(\hat{R}_{o,AB})$, and $N_{\Psi_A}(\mathcal{C})$ denotes the number of points of Ψ_A in the region $\mathcal{C}$. Based on the above discussion, in the following Lemma, we present the expression for K_2, which is the CDF of $R_{o,AB}$ conditioned on the distances R_o^A, R_o^B, and Event-2.

Lemma 3: The CDF *of the distance* $R_{o,AB}$ *conditioned on distances* R_o^A, R_o^B, *and Event-2 is given as* $F_{R_{o,AB}}(r_{o,AB}|\, r_o^A, r_o^B, E_2(r_o^B)) =$

$$
\begin{aligned}
&\mathbb{P}\Big[R_{o,AB} \le r_{o,AB}\Big|r_o^A, r_o^B, E_2(r_o^B)\Big]\\
&\quad= 1 - \mathbb{E}_{\Theta_A}\Big[\mathbf{1}(\hat{R}_{o,AB} > r_{o,AB})\exp(-\lambda_A|\mathcal{C}_1(\hat{R}_{o,AB})|)\Big],
\end{aligned}
\tag{27}
$$

where

$$
\begin{aligned}
&f_{\Theta_A}(\theta_A|r_o^A, r_o^B, E_2(r_o^B))\\
&\quad= \frac{1}{2\varphi_{AB}(r_o^A, r_o^B, R_{pz})}, \quad |\theta_A| \le \varphi_{AB}(r_o^A, r_o^B, R_{pz}),
\end{aligned}
\tag{28}
$$

and $\varphi_{AB}(r_o^A, r_o^B, R_{pz}) =$

$$\begin{cases} \pi & r_o^B - R_{pz} \ge r_o^A,\ r_o^B \ge R_{pz}, \\ \arccos\left(\dfrac{(r_o^A)^2 + (r_o^B)^2 - R_{pz}^2}{2r_o^A r_o^B}\right) & |r_o^B - R_{pz}| < r_o^A \le r_o^B + R_{pz}, \\ \pi & r_o^B + R_{pz} \le r_o^A. \end{cases} \tag{29}$$

Proof: Please refer to Appendix B. ■

Our next objective is to get the conditional density functions of R_o^A presented in (23). Hence, in the following Lemma, taking both the events discussed in Section III-A2 into account, we derive a lower bound on the CDF of R_o^A conditioned on R_o^B.

Lemma 4: Conditioned on the distance R_o^B *between the tagged OpB BS and the typical user, the* CDF *of the distance* R_o^A *between the typical user and its nearest*

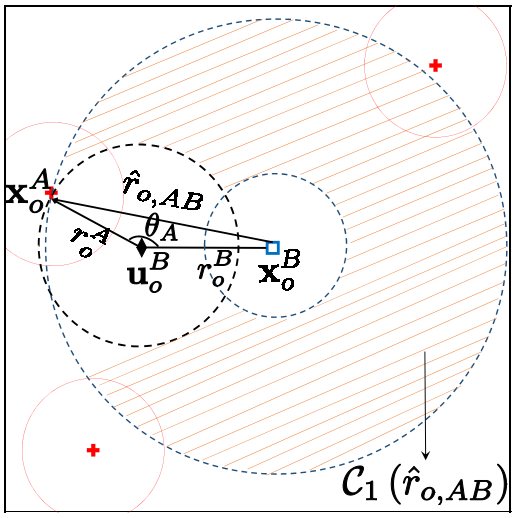

(a)

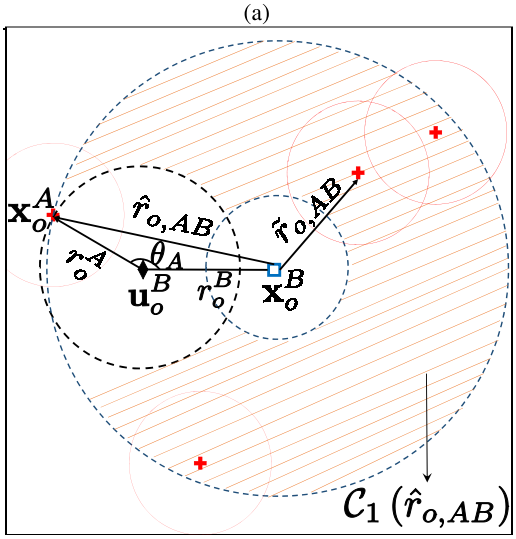

(b)

FIGURE 6. The diamond, crosses, and squares represent the locations of the typical OpB user, OpA BSs, and OpB BSs, respectively. The location of the typical user is $\mathbf{u}_o^B = (0, 0)$ and the tagged OpB BS is $\mathbf{x}_o^B = (r_o^B, 0)$.

OpA BS is $F_{R_o^A}(r_o^A|r_o^B) \geq F_{R_o^A}^{\mathrm{LB}}(r_o^A|r_o^B) =$

$$\left(1-\exp(-\mathcal{G}(r_o^A,\lambda_A,R_{pz},r_o^B))\right)\frac{\exp(-\pi\lambda_B(r_o^B)^2)}{1-F_{R_o^B}(r_o^B)} + F_{R_o^A}^{\mathrm{LB}}(r_o^A|r_o^B,E_1(r_o^B))\left(1-\frac{\exp(-\pi\lambda_B(r_o^B)^2)}{1-F_{R_o^B}(r_o^B)}\right). \quad (30)$$

In the above equation $F_{R_o^A}^{\mathrm{LB}}(r_o^A|r_o^B,E_1(r_o^B)) =$

$$\begin{cases} 0 & r_o^A + r_o^B \leq R_{pz} \\ \min\left(1, \frac{1-\exp(-\lambda_A|\mathcal{C}_2(r_o^A,r_o^B,R_{pz})|)}{1-\exp(-\lambda_A|\mathcal{C}_2(r_o^B+R_{pz},r_o^B,R_{pz})|)}\right) & r_o^A + r_o^B > R_{pz}, \end{cases} \quad (31)$$

where $\mathcal{C}_2(r_o^A, r_o^B, R_{pz}) = \mathcal{B}_{r_o^A}(\mathbf{u}_o^B) \setminus \{\mathcal{B}_{r_o^A}(\mathbf{u}_o^B) \cap \mathcal{B}_{R_{pz}}(\mathbf{x}_o^B)\}$. *Corresponding* PDF $f_{R_o^A}^{\mathrm{LB}}(r_o^A|r_o^B)$ *is obtained by differentiating* $F_{R_o^A}^{\mathrm{LB}}(r_o^A|r_o^B)$ *w.r.t.* r_o^A. $F_{R_o^B}(r_o^B)$ *is the* CDF *of the contact distance of PHP.*

Proof: Please refer to Appendix C. ■

While above lower bound captures the effect of both Event-1 and Event-2, as we will see later this bound on the CDF of R_o^A results in a relatively loose bound for the CDF of $R_{o,AB}$. Hence, our next objective is to present an accurate approximate expression for R_o^A conditioned on R_o^B. Observe that when the typical user is farther from tagged BS, the average area of overlap between a protection zone (whose center is uniformly distributed over the region $\mathcal{B}_{R_o^B+R_{pz}}(\mathbf{u}_o^B) \setminus \mathcal{B}_{R_{pz}}(\mathbf{x}_o^B)$) and the the circle $\mathcal{B}_{R_o^B}(\mathbf{u}_o^B)$ is relatively small. Hence, the average number of OpA BSs required in $\mathcal{B}_{R_o^B+R_{pz}}(\mathbf{u}_o^B)$ to ensure that all the points of Ψ_B in $\mathcal{B}_{R_o^B}(\mathbf{u}_o^B)$ are deleted is likely to be larger than one. Considering the above observation, in the following Lemma, we present an approximate expression for the CDF of R_o^A conditioned on the distance R_o^B.

Lemma 5: Conditioned on the distance R_o^B *between the tagged OpB BS and the typical user, the approximate* CDF *of the distance* R_o^A *between the typical user and its nearest OpA BS is given as*

$$\begin{aligned} &F_{R_o^A}(r_o^A|r_o^B) \\ &= \mathbb{P}\left[R_o^A \leq r_o^A | N_{\Phi_B}(\mathcal{B}_{r_o^B}(\mathbf{u}_o^B)) = 0, r_o^B\right] \\ &= 1-\exp(-\mathcal{G}(r_o^A,\lambda_A,R_{pz},r_o^B))\frac{\exp(-\pi\lambda_B(r_o^B)^2)}{1-F_{R_o^B}(r_o^B)} \\ &\quad + F_{R_o^A}(r_o^A|r_o^B,E_1(r_o^B))\left(1-\frac{\exp(-\pi\lambda_B(r_o^B)^2)}{1-F_{R_o^B}(r_o^B)}\right), \end{aligned} \quad (32)$$

where approximate expression is obtained by replacing $F_{R_o^A}(r_o^A|r_o^B, E_1(r_o^B))$ *by the expression presented in* (35) *at the top of the next page. Corresponding conditional* PDF *of* R_o^A *is* $f_{R_o^A}(r_o^A|r_o^B) =$

$$\begin{aligned} &f_{R_o^A}(r_o^A|r_o^B,E_2(r_o^B))\frac{\exp(-\pi\lambda_B(r_o^B)^2)}{1-F_{R_o^B}(r_o^B)} \\ &\quad + f_{R_o^A}(r_o^A|r_o^B,E_1(r_o^B))\left(1-\frac{\exp(-\pi\lambda_B(r_o^B)^2)}{1-F_{R_o^B}(r_o^B)}\right), \end{aligned} \quad (33)$$

where

$$\begin{aligned} &f_{R_o^A}(r_o^A|r_o^B,E_2(r_o^B)) \\ &\quad = 2\pi\mathcal{E}(r_o^A,\lambda_A,R_{pz},r_o^B)r_o^A\exp(-\mathcal{G}(r_o^A,\lambda_A,R_{pz},r_o^B)). \end{aligned} \quad (34)$$

The approximate expression for the PDF *is obtained by replacing* $f_{R_o^A}(r_o^A|r_o^B, E_1(r_o^B))$ *by the derivative of* $F_{R_o^A}(r_o^A|r_o^B, E_1(r_o^B))$ *in* (35). *Further, the complementary* CDF *of* R_o^B *in the denominator is replaced by the approximate expression in* (80). *The expressions for* $\mathcal{E}(r_o^A, \lambda_A, R_{pz}, r_o^B)$ *and* $\mathcal{G}(r_o^A, \lambda_A, R_{pz}, r_o^B)$ *were presented in Lemma 1.*

Proof: Please refer to Appendix D. ■

$$F_{R_o^A}(r_o^A|r_o^B, E_1(r_o^B)) \approx \begin{cases} 0 & r_o^A + r_o^B \le R_{pz} \\ \dfrac{1-\exp(-\lambda_A\pi((r_o^A)^2-(R_{pz}-r_o^B)^2))}{1-\exp(-\lambda_A\pi((R_{pz}+r_o^B)^2-(R_{pz}-r_o^B)^2))} & r_o^B \le R_{pz}/2, R_{pz}-r_o^B < r_o^A \le R_{pz}+r_o^B \\ \dfrac{1-\exp\left(-\lambda_A\pi\left((r_o^A)^2-\max(0,R_{pz}-r_o^B)^2\right)\right)}{1-\exp(-\lambda_A\pi((r_o^B)^2-\max(0,R_{pz}-r_o^B)^2))} & R_{pz}/2 < r_o^B, \max(0,R_{pz}-r_o^B) < r_o^A \le r_o^B. \end{cases} \quad (35)$$

In the following Lemma, using Lemmas 3 and 4, we derive a lower bound for the CDF of $R_{o,AB}$.

Lemma 6: The CDF of the distance $R_{o,AB}$ between the tagged BS and its nearest OpA BS is lower bounded by $F_{R_{o,AB}}(r_{o,AB}) \ge F^{(\mathrm{LB},1)}_{R_{o,AB}}(r_{o,AB}) =$

$$\int_0^\infty \int_{\max(0,R_{pz}-r_o^B)}^\infty F_{R_{o,AB}}(r_{o,AB}|r_o^A, r_o^B, E_2(r_o^B)) f^{\mathrm{LB}}_{R_o^A}(r_o^A|r_o^B) f_{R_o^B}(r_o^B) \mathrm{d}r_o^A \, \mathrm{d}r_o^B, \quad (36)$$

where $F_{R_{o,AB}}(r_{o,AB}|r_o^A, r_o^B, E_2(r_o^B))$ is given by (27), *$f^{\mathrm{LB}}_{R_o^A}(r_o^A|r_o^B)$ is obtained by differentiating $F^{\mathrm{LB}}_{R_o^A}(r_o^A|r_o^B)$ w.r.t. r_o^A presented in Lemma 4, and $f_{R_o^B}(r_o^B)$ is the PDF of the contact distance distribution of PHP.*

Note that accurate evaluation of the above lower bound requires the exact expression for the CDF of R_o^B. Now, using Lemmas 3, and 5, we derive an approximate expression for the CDF of $R_{o,AB}$, which is presented next.

Lemma 7: The CDF of the distance $R_{o,AB}$ conditioned on R_o^B is given as $F_{R_{o,AB}}(r_{o,AB}|r_o^B) \approx$

$$\int_{\max(0,R_{pz}-r_o^B)}^\infty F_{R_{o,AB}}(r_{o,AB}|r_o^A, r_o^B, E_2(r_o^B)) f_{R_o^A}(r_o^A|r_o^B) \, \mathrm{d}r_o^A, \quad (37)$$

where $F_{R_{o,AB}}(r_{o,AB}|r_o^A, r_o^B, E_2(r_o^B))$ is given by (27) *and $f_{R_o^A}(r_o^A|r_o^B)$ is given by* (33).

The marginal distribution of $R_{o,AB}$ can be obtained by deconditioning the above expression w.r.t. R_o^B whose PDF can be approximated as Weibull distribution (Refer to Section II).

The expressions for lower bound and approximate CDF presented in (36) and (37) are not in closed form and require a fair amount of computational resource for evaluation. In the following Lemma, considering only Event-2 discussed in Section III-A2, we present another lower bound on the CDF of $R_{o,AB}$ that assumes a closed form expression.

Lemma 8: The lower bound on the CDF of the distance $R_{o,AB}$ between the tagged OpB BS and its nearest OpA BS is

$$F_{R_{o,AB}}(r_{o,AB}) \ge F^{(\mathrm{LB},2)}_{R_{o,AB}}(r_{o,AB}) = 1 - \exp\left(-\pi\lambda_A((r_{o,AB})^2 - R_{pz}^2)\right),$$

which is a truncated Rayleigh distribution.

Proof: Please refer to Appendix E. ∎

3) APPROXIMATE AND LOWER BOUND EXPRESSIONS FOR THE MAP OF THE TAGGED BS

Based on the distance distributions of $R_{o,AB}$ presented in the previous subsection, in this subsection, we present lower bound and approximated expressions for the MAP of the tagged BS.

First, using the approximate conditional CDF of $R_{o,AB}$ presented in Lemma 7, we derive an approximate expression for the MAP of the tagged BS, which is presented in the following Lemma.

Lemma 9: The MAP of the tagged OpB BS located at $\mathbf{x}_o^B \in \Phi_B$ is given as $\mathcal{M}_o^B = \mathbb{P}\left[\mathcal{I}_o^B = 1\right] \approx$

$$\int_{r_o^B=0}^\infty \mathrm{d}r_o^B \int_{r_o^A=\max(0,R_{pz}-r_o^B)}^\infty \mathrm{d}r_o^A \int_{r_{o,AB}=R_{pz}}^\infty \frac{1-e^{-f_1(r_{o,AB},r_o^B)}}{f_1(r_{o,AB},r_o^B)} \times \mathrm{d}F_{R_{o,AB}}(r_{o,AB}|r_o^A, r_o^B, E_2(r_o^B)) f_{R_o^A}(r_o^A|r_o^B) f_{R_o^B}(r_o^B), \quad (38)$$

where $F_{R_{o,AB}}(r_{o,AB}|r_o^A, r_o^B, E_2(r_o^B))$ is given by (27), *$f_{R_o^A}(r_o^A|r_o^B)$ is given by* (33), *and $f_{R_o^B}(r_o^B)$ is given in* (4).

Proof: The proof follows from deconditioning (20) in Lemma 2 w.r.t. $R_{o,AB}$ and R_o^B. Above expression for the MAP can be evaluated using numerical integration technique such as Monte-Carlo integration. ∎

Now, instead of the approximate expression, if we consider any of the lower bound expressions on the CDF to decondition the MAP in (20), then we obtain a lower bound on the MAP of the tagged BS. Intuitively this is justified as follows: considering a lower bound on the CDF of the distance implies that on an average, the distance to the nearest PZ center is relatively larger than the actual distance. As a result, in the contention domain of the tagged BS, relatively closer points in Ψ_B are considered during the evaluation of MAP. Based on this observation, in the following Lemma, we present a lower bound expression for the MAP of the tagged BS.

Lemma 10: A lower bound on the MAP of the tagged OpB BS located at $\mathbf{x}_0^B \in \Phi_B$ is given as $\mathcal{M}_o^B = \mathbb{P}\left[\mathcal{I}_o^B = 1\right] \ge$

$$\int_{r_o^B=0}^\infty \int_{r_{o,AB}=R_{pz}}^\infty \frac{1-\exp(-f_1(r_{o,AB},r_o^B))}{f_1(r_{o,AB},r_o^B)} \mathrm{d}F^{(\mathrm{LB},\mathrm{x})}_{R_{o,AB}}(r_{o,AB}|r_o^B) f_{R_o^B}(r_o^B) \mathrm{d}r_o^B, \quad (39)$$

where $f_{R_o^B}$ is the PDF of the contact distance of PHP. Above expression can be evaluated using either of the

lower bound expressions for the CDF *of* $R_{o,AB}$ *presented in Lemmas 6 and 8.*

Proof: Please refer to Appendix F. ■

In Fig. 7, the CDFs of $R_{o,AB}$ obtained from Lemmas 6, 8, and 7 are compared with simulation results for two different combinations of λ_A and λ_B. Note that to obtain the lower bound on the CDF of $R_{o,AB}$ using Lemma 6, we need the exact CDF of R_o^B in (30). As mentioned earlier, due to unavailability the exact expression for the CDF, we have used the approximated cumulative CDF of R_o^B given in (80). On the other hand, since the density of OpA BS λ_A is fixed in both the cases, the lower bounds obtained using Lemma 8 are the same irrespective of the value of λ_B. The results on the tightness of the lower bounds and accuracy of the approximated MAP expression are presented in Section VI.

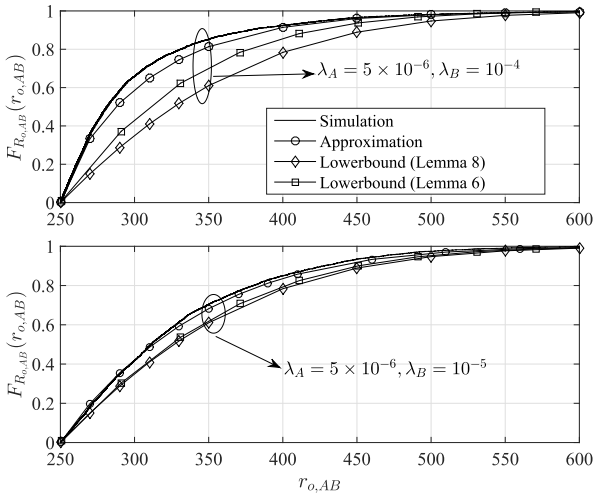

FIGURE 7. CDF **of the distance between the tagged BS and its nearest OpA BS.**

IV. COVERAGE PROBABILITY FOR A TYPICAL OpB USER

Due to the consideration of Rayleigh fading, the small-scale channel gain in the desired link follows exponential distribution. Hence, the coverage probability of the typical user can be readily expressed in terms of the LT of aggregate interference [12]. However, in this case, *exact* characterization of the LT of aggregate interference is not trivial because of the following reasons:

1. Based on our discussion in Section III-A2, conditioned on the distance between the tagged BS and the typical user, characterizing the distance distribution between the typical user and its nearest OpA interfering BS is not trivial.

2. Due to the presence of PZs around each OpA BS, there is dependency in the locations of OpA and OpB BSs. This dependency leads to correlation in the interference power perceived at the typical user from both sets of BSs. In addition, characterizing the interference contribution from OpB BSs while taking the PZs into account is not trivial.

3. Conditioned on the event that the tagged BS is always active, the MAP of the interfering OpB BSs in Φ_B gets affected, i.e. any OpB BS in the contention domain of the tagged OpB BS remains inactive, which affects the interference field.

Circumventing the above problems, we provide fairly accurate expression for the LT of interference using the following steps:

1. Note that in the previous section, we have already addressed the first problem. In Lemma 5, we have presented an approximate expression for the CDF of the R_o^A conditioned on R_o^B.

2. To capture the correlation in the interference powers from the BSs in the vicinity of the typical user, we determine the density of interfering OpA BSs conditioned on R_o^B and R_o^A (Refer to Lemma 11). Further, we approximate the PHP Φ_B by a non-homogeneous PPP conditioned on R_o^A and R_o^B (Refer to Lemma 12).

3. We obtain the MAP of an interfering OpB BS conditioned on the event that the tagged OpB BS is active (Refer to Lemma 13). This conditional MAP provides the retention probability of an interfering BS in Φ_B.

A flow diagram of the above sequence of steps is presented in Fig. 8.

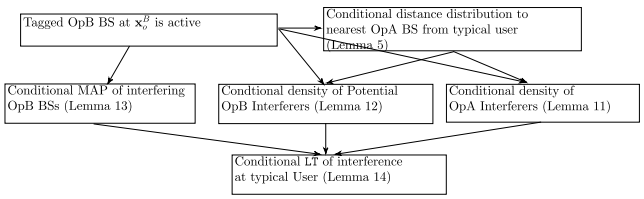

FIGURE 8. **Sequence of steps to obtain the** LT **of aggregate interference at the typical OpB user conditioned on the distance to the tagged BS and the nearest OpA interfering user.**

1) CONDITIONAL DENSITY OF INTERFERING OpA BSs

As per the assumption made in the system model, the locations of the interfering OpA BSs follow a homogeneous PPP of density λ_A. However, due to the presence of exclusion zone $\mathcal{B}_{R_{pz}}(\mathbf{x}_o^B)$, the density of OpA BS is zero in $\mathcal{B}_{R_{pz}}(\mathbf{x}_o^B)$. As mentioned in Section III-A2, conditioned on the distance R_o^B, the density of OpA BSs in the vicinity of the typical user is dictated by both Event-1 and Event-2. Since characterizing the density of Ψ_A conditioned on Event-1 is difficult, we only take into account Event-2 to obtain the density of Ψ_A. In the following Lemma, we present this conditional density of interfering OpA BSs.

Lemma 11: Conditioned on the distances R_o^B *and* R_o^A, Ψ_A *is characterized as a non-homogeneous PPP with the density function*

$$\tilde{\lambda}_{\Psi_A}(x|r_o^B, r_o^A) = \mathcal{E}(x, \lambda_A, R_{pz}, r_o^B)\mathbf{1}(x > r_o^A) \tag{40}$$

where $\mathcal{E}$ *is given by* (18) *in Lemma 1.*

Proof: Let $\mathbf{x}_o^B$ be the location of the tagged BS and $r_o^B = \|\mathbf{x}_o^B\|$. Since the tagged OpB BS is active, there are no interfering OpA BSs in $\mathcal{B}_{R_{pz}}(\mathbf{x}_o^B)$, i.e. $\mathcal{B}_{R_{pz}}(\mathbf{x}_o^B)$ is a hole in

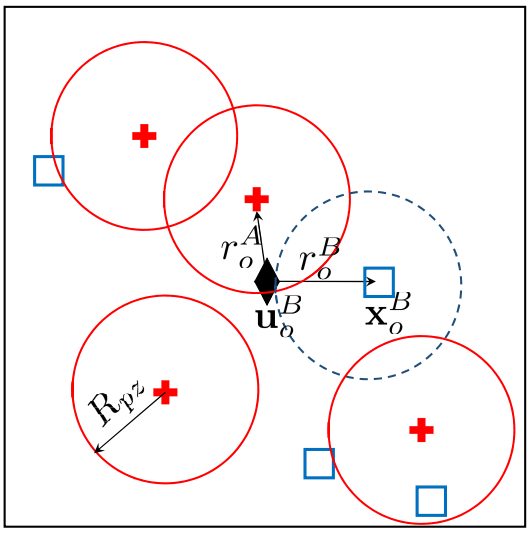

(a)

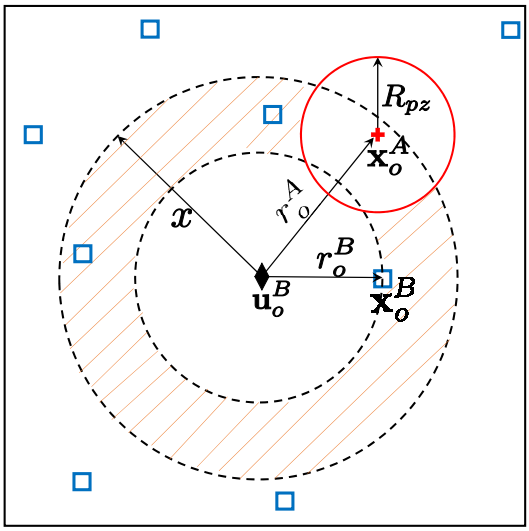

(b)

FIGURE 9. The diamond, crosses, and squares represent the locations of the typical OpB user, OpA BSs, and OpB BSs, respectively. The location of the typical user is $\mathbf{u}_o^B = (0, 0)$ and the tagged OpB BS is $\mathbf{x}_o^B = (r_o^B, 0)$. (a) An illustration for Lemma 11. (b) A representative diagram for Lemma 12.

the PPP Ψ_A (See Fig. 9a). Hence, the density function given in (40) follows directly from the application of Lemma 1 and the fact that all the interfering BSs are at a distance greater than r_o^A from the typical user. ■

In Section VI, we verify through Monte Carlo simulations that the effect of above approximation is negligible on the coverage probability result. Note that the aggregate interference is dictated by the most dominant interference term (cf. [18] for a simulation based verification). In this case, the interference contribution from the nearest OpA BS, which is likely to be the most dominant interferer, is captured reasonably accurately. This leads to fairly accurate approximation of total interference from the OpA BSs.

2) APPROXIMATION OF Φ_B AS A NON-HOMOGENEOUS PPP

As discussed earlier, since the PGFL of a PHP is not known, characterizing the LT of aggregate interference from the BSs in Φ_B is not trivial. Hence, we approximate the PHP Φ_B by a non-homogeneous PPP. First, we consider the parent PPP Ψ_B and determine its density function taking into account the nearest PZ to the typical user [23]. Then, to capture the effect of rest of the PZs in the network, we introduce independent thinning of points in Ψ_B beyond the nearest OpA BS. Based on the above discussion, conditioned on R_o^A and R_o^B, we characterize the density of Φ_B, which is presented next.

Lemma 12: Conditioned on the distances R_o^A and R_o^B, we approximate Φ_B as a non-homogeneous PPP with piece-wise density function given as

$$\tilde{\lambda}_{\Psi_B}(x|r_o^A, r_o^B) = \frac{1}{2\pi x}\frac{\mathrm{d}\Lambda_{\Psi_B}\left(\mathcal{B}_x(\mathbf{o})|r_o^A, r_o^B\right)}{\mathrm{d}x}\exp(-\pi\lambda_A R_{pz}^2\mathbf{1}(x \geq r_o^A)), \tag{41}$$

where $\Lambda_{\Psi_B}\left(\mathcal{B}_x(\mathbf{o})|r_o^A, r_o^B\right) = \mathcal{H}(x, r_o^A, r_o^B, R_{pz})$ is the conditional intensity measure of the PPP Ψ_B and $\mathcal{H}$ is given in (42) *at the top of the next page.*

Proof: Let $\mathbf{x}_o^A \in \Psi_A$ and $\mathbf{x}_o^B \in \Phi_B$ be the locations of the nearest OpA BS to the typical user and the tagged OpB BS, respectively. Further, $r_o^A = \|\mathbf{x}_o^A\|$ and $r_o^B = \|\mathbf{x}_o^B\|$. This Lemma can be proved in two steps. In the first step, we consider the baseline PPP Ψ_B from which Φ_B is obtained. Considering only the nearest PZ and the distance to the tagged BS, the conditional intensity measure of Ψ_B is the average number of points in the region

$$\mathcal{C}_3(x, \mathbf{x}_o^B, \mathbf{x}_o^A, R_{pz}) = \mathcal{B}_x(\mathbf{u}_o^B) \setminus \{\mathcal{B}_{r_o^B}(\mathbf{u}_o^B) \cup \mathcal{B}_{R_{pz}}(\mathbf{x}_o^A)\}, \tag{43}$$

which is illustrated as the shaded region in Fig. 9b. Hence, the conditional intensity measure of Ψ_B is given as

$$\Lambda_{\Psi_B}\left(\mathcal{B}_x(\mathbf{o})|r_o^A, r_o^B\right) = \lambda_B|\mathcal{C}_3(x, \mathbf{x}_o^B, \mathbf{x}_o^A, R_{pz})|, \tag{44}$$

where $|\mathcal{C}|$ denotes the area of the region $\mathcal{C}$. $\mathbf{u}_o^B$ and $\mathbf{o}$ are interchangeably used as it is assumed that the typical user is located at the origin. Depending on the relative distances r_o^A, r_o^B, and x, the conditional intensity measure is a piecewise function given in (42). Now, the corresponding conditional density function of Ψ_B is

$$\lambda_{\Psi_B}(x|r_o^A, r_o^B) = \frac{1}{2\pi x}\frac{\mathrm{d}\Lambda_{\Psi_B}\left(\mathcal{B}_x(\mathbf{o})|r_o^A, r_o^B\right)}{\mathrm{d}x}. \tag{45}$$

In the second step, to account for the rest of the PZs in the network, independent thinning of the BS locations in Ψ_A beyond the nearest OpA BS is performed. Combining both the steps, we get the conditional density function of Φ_B in (41). ■

3) CONDITIONAL MAP OF THE INTERFERING OpB BSs

Except the tagged BS, each BS in Φ_B acts as a potential interfering BS, but only those BSs who win contention w.r.t.

$$\mathcal{H}(x, r_o^A, r_o^B, R_{pz}) = \begin{cases} \lambda_B \pi (x^2 - (r_o^B)^2) & r_o^A + R_{pz} < r_o^B \\ \lambda_B (\pi (x^2 - (r_o^B)^2) - A(x, R_{pz}, r_o^A) + A(r_o^B, R_{pz}, r_o^A)) & r_o^B - R_{pz} < r_o^A < r_o^B + R_{pz}, r_o^B \le x \le r_o^A + R_{pz} \\ \lambda_B \pi (x^2 - (r_o^B)^2 - R_{pz}^2 + \dfrac{A(r_o^B, R_{pz}, r_o^A)}{\pi}) & r_o^B - R_{pz} < r_o^A < r_o^B + R_{pz}, x \ge r_o^A + R_{pz} \\ \lambda_B \pi (x^2 - (r_o^B)^2) & r_o^A > r_o^B + R_{pz}, x < r_o^A - R_{pz} \\ \lambda_B \pi (x^2 - ((r_o^B)^2 + \dfrac{A(x, R_{pz}, r_o^A)}{\pi})) & r_o^A > r_o^B + R_{pz}, r_o^A - R_{pz} \le x \le r_o^A + R_{pz} \\ \lambda_B \pi (x^2 - (r_o^B)^2 - R_{pz}^2) & r_o^A > r_o^B + R_{pz}, x > r_o^A + R_{pz}, \end{cases} \tag{42}$$

where $A(r, R, d)$ is defined in (17) and $x > r_o^B$.

other OpB BSs in Φ_B will actually interfere. However, this contention process is conditioned on the event that the tagged OpB BS is always active. In the following Lemma, we derive the conditional MAP of an interfering BS located at $\mathbf{x}_i^B \in \Phi_B$.

Lemma 13: Conditioned on the event that the tagged OpB BS at $\mathbf{x}_o^B = (r_o^B, 0)$ *is active, the conditional* MAP *of an interfering OpB BS located at* $\mathbf{x}_i^B = (\|\mathbf{x}_i^B\| \cos(\theta_{x_i^B}), \|\mathbf{x}_i^B\| \sin(\theta_{x_i^B})) \in \Phi_B$ *is given as* $M(\mathbf{x}_i^B | r_o^B) =$

$$\frac{f_3(r_o^B, \mathbf{x}_o^B)}{1 - e^{-f_3(r_o^B, \mathbf{x}_o^B)}} \left[\frac{1 - e^{-f_3(r_o^B, \mathbf{x}_i^B)}}{f_3(r_o^B, \mathbf{x}_i^B)} - \frac{1 - e^{-f_4(r_o^B, \mathbf{x}_i^B)}}{f_4(r_o^B, \mathbf{x}_i^B)} \right] \times \frac{2(1 - \exp\left(-\frac{\tau_{cs} l(\|\mathbf{x}_o^B - \mathbf{x}_i^B\|)}{P_B}\right))}{\left(f_4(r_o^B, \mathbf{x}_i^B) - f_3(r_o^B, \mathbf{x}_i^B)\right)}, \tag{46}$$

where

$$f_3(r_o^B, \mathbf{x}_i^B) = \int_{x=r_0^B}^{\infty} \int_{\theta_x=0}^{2\pi} \lambda_B \times e^{-\frac{\tau_{cs} l\left(\sqrt{x^2 + \|\mathbf{x}_i^B\|^2 - 2x\|\mathbf{x}_i^B\| \cos(\theta_x - \theta_{x_i^B})}\right)}{P_B}} \mathrm{d}\theta_x x \mathrm{d}x, \tag{47}$$

and $f_4(r_o^B, \mathbf{x}_i^B) =$

$$\int_{x=r_o^B}^{\infty} \int_{\theta_x=0}^{2\pi} \lambda_B \times \left(1 - \left(1 - e^{-\frac{\tau_{cs} l\left(\sqrt{x^2 + (r_o^B)^2 - 2x r_o^B \cos(\theta_x)}\right)}{P_B}}\right) \times \left(1 - e^{-\frac{\tau_{cs} l\left(\sqrt{x^2 + \|\mathbf{x}_i^B\|^2 - 2x\|\mathbf{x}_i^B\| \cos(\theta_x - \theta_{x_i^B})}\right)}{P_B}}\right)\right) \mathrm{d}\theta_x x \mathrm{d}x. \tag{48}$$

Proof: This proof follows on the same lines as that of [14, Proposition 2]. Here, we provide a brief sketch. The main assumption that we have made in this case is to ignore the effect of all the PZs. Let $\mathcal{I}_o^B$ and $\mathcal{I}_j^B$ be the medium access indicators of the tagged BS and the OpB BS located at $\mathbf{x}_j^B$. Now,

$$\mathbb{P}\left[\mathcal{I}_j^B = 1 \middle| \mathcal{I}_o^B = 1, r_o^B\right] = \frac{\mathbb{P}\left[\mathcal{I}_j^B = 1, \mathcal{I}_o^B = 1 \middle| r_o^B\right]}{\mathbb{P}\left[\mathcal{I}_o^B = 1 \middle| r_o^B\right]}. \tag{49}$$

From [14, Proposition 2], $\mathbb{P}\left[\mathcal{I}_j^B = 1, \mathcal{I}_o^B = 1 \middle| r_o^B\right] =$

$$\left[\frac{1 - \exp(-f_3(r_o^B, \mathbf{x}_i^B))}{f_3(r_o^B, \mathbf{x}_i^B)} - \frac{1 - \exp(-f_4(r_o^B, \mathbf{x}_i^B))}{f_4(r_o^B, \mathbf{x}_i^B)}\right] \times \frac{2\left(1 - \exp\left(-\frac{\tau_{cs} l(\|\mathbf{x}_o^B - \mathbf{x}_i^B\|)}{P_B}\right)\right)}{\left(f_4(r_o^B, \mathbf{x}_i^B) - f_3(r_o^B, \mathbf{x}_i^B)\right)}, \tag{50}$$

and

$$\mathbb{P}\left[\mathcal{I}_o^B = 1 \middle| r_o^B\right] = \frac{1 - \exp(-f_3(r_o^B, \mathbf{x}_o^B))}{f_3(r_o^B, \mathbf{x}_o^B)}. \tag{51}$$

Replacing (50) and (51) in (49), we obtain $M(\mathbf{x}_i^B | r_o^B)$ presented in the Lemma. ■

A. LT OF INTERFERENCE AND COVERAGE PROBABILITY

Using Lemmas 11, 12, and 13, we derive the LT of interference at the typical OpB user conditioned on its distance to the tagged OpB BS and the nearest OpA BS.

Lemma 14: The approximate LT *of aggregate interference at the typical user conditioned on the distances* R_o^A *and* R_o^B *is given as* $\mathcal{L}_{I_{agg}^B}(s | r_o^A, r_o^B, \mathcal{I}_o^B = 1) =$

$$\mathcal{L}_{I_{agg}^{BA}}(s | r_o^A, r_o^B) \mathcal{L}_{I_{agg}^{BB}}(s | r_o^A, r_o^B, \mathcal{I}_o^B = 1), \tag{52}$$

where I_{agg}^{BA} *and* I_{agg}^{BB} *represent the total interference at the OpB typical user from the OpA and OpB BSs, respectively. In the above equation,*

$$\mathcal{L}_{I_{agg}^{BB}}(s | r_o^A, r_o^B, \mathcal{I}_o^B = 1) = \exp\left(-\int_{x=r_o^B}^{\infty} \int_{\theta=0}^{2\pi} \frac{\tilde{\lambda}_{\Psi_B}(x | r_o^A, r_o^B) M(\mathbf{x}(x, \theta) | r_o^B)}{l(x)(sP_B)^{-1} + 1} \mathrm{d}\theta x \mathrm{d}x\right), \tag{53}$$

and

$$\mathcal{L}_{I_{agg}^{BA}}(s | r_o^A, r_o^B) = \frac{1}{1 + \frac{sP_A}{l(r_o^A)}} \exp\left(-2\pi \int_{y=r_o^A}^{\infty} \frac{\tilde{\lambda}_{\Psi_A}(y | r_o^A, r_o^B)}{l(y)(sP_A)^{-1} + 1} y \mathrm{d}y\right). \tag{54}$$

Proof: Please refer to Appendix G. ∎

Next, using the LT of interference, we derive the SIR coverage probability for a typical OpB user in the following Proposition.

Proposition 1: The SIR *coverage probability for a typical OpB user at the origin is given as* $\mathtt{P}_{\mathtt{C}}^{(\mathtt{B})}(T) =$

$$\int_{r_o^B=0}^{\infty}\int_{r_o^A=0}^{\infty}\mathcal{L}_{I_{agg}^B}\left(\frac{Tl(r_o^B)}{P_B}\middle| r_o^A, r_o^B, \mathcal{I}_o^B=1\right) f_{R_o^A}(r_o^A|r_o^B) \times f_{R_o^B}(r_o^B)\mathrm{d}r_o^A\mathrm{d}r_o^B, \tag{55}$$

where the $f_{R_o^B}(r_o^B)$ *and* $f_{R_o^A}(r_o^A|r_o^B)$ *are given by* (4) *and* (33)*, respectively.*

Proof: Conditioned on the distances R_o^A and R_o^B, the SIR coverage probability is given as

$$\begin{aligned}
&\mathbb{P}\left[\frac{P_B h}{l(r_o^B)I_{agg}^B} > T\middle| r_o^A, r_o^B, \mathcal{I}_o^B=1\right]\\
&= \mathbb{P}\left[h > \frac{Tl(r_o^B)I_{agg}^B}{P_B}\middle| r_o^A, r_o^B, \mathcal{I}_o^B=1\right]\\
&= \mathbb{E}\left[\exp\left(-\frac{Tl(r_o^B)I_{agg}^B}{P_B}\right)\middle| r_o^A, r_o^B, \mathcal{I}_o^B=1\right]\\
&= \mathcal{L}_{I_{agg}^B}\left(\frac{Tl(r_o^B)}{P_B}\middle| r_o^A, r_o^B, \mathcal{I}_o^B=1\right),
\end{aligned} \tag{56}$$

where the last step follows from the definition of the LT. The expression for the LT is presented in Lemma 14. Since the expression only depends on the distances R_o^B and R_o^A, the final coverage probability expression is obtained by deconditioning the LT using joint distribution of R_o^A and R_o^B. ∎

V. COVERAGE PROBABILITY FOR A TYPICAL OpA USER

In this section, we present the coverage probability expression for a typical OpA user, who is served by the nearest OpA BS (the tagged OpA BS). Similar to the approach followed in the previous section, we capture the correlation in the interference powers from OpA and OpB BSs in the vicinity of the typical user. In addition, we evaluate the LT of interference from OpB BSs following the similar method as described in the previous section. Most of the theoretical expressions presented in this section such as conditional density of interferers can be proved on the similar lines of the proofs presented in the previous section. Hence, to avoid repetitions, instead of providing detailed proofs we just present proof sketches.

A. APPROXIMATION OF Φ_B AS A NON-HOMOGENEOUS PPP

To begin with, in the following Lemma, we approximate the PHP Φ_B by a non-homogeneous PPP and derive its density function conditioned on the distance between the typical OpA user and the tagged OpA BS.

Lemma 15: Conditioned on the serving distance R_o^A *between the typical user and the tagged OpA BS,* Φ_B *is approximated as a non-homogeneous PPP with density function* $\tilde{\lambda}_{\Psi_B}(x|r_o^A) =$

$$\frac{1}{2\pi x}\frac{\mathrm{d}\Lambda_{\Psi_B}\left(\mathcal{B}_x(\mathbf{o})|r_o^A\right)}{\mathrm{d}x}\exp(-\pi\lambda_A R_{pz}^2\mathbf{1}(x\geq r_o^A)), \tag{57}$$

where $\Lambda_{\Psi_B}\left(\mathcal{B}_x(\mathbf{o})|r_o^A\right) = \mathcal{G}(x,\lambda_B,R_{pz},r_o^A)$ *is the conditional intensity measure of the PPP* Ψ_B *and* $\mathcal{G}$ *is defined in Lemma 1.*

Proof: Proof of this Lemma can be done on the similar lines as that of Lemma 12. Let the tagged OpA BS is located at $\mathbf{x}_o^A$ and $r_o^A = \|\mathbf{x}_o^A\|$. In the first step, we obtain the intensity measure of Ψ_B conditioned on the location of the nearest PZ $\mathcal{B}_{R_{pz}}(\mathbf{x}_o^A)$ to the typical user (Refer Fig. 2a). Since we are considering only the nearest PZ, i.e. $\mathcal{B}_{R_{pz}}(\mathbf{x}_o^A)$, the conditional intensity measure is obtained directly by applying Lemma 1 and is given as

$$\Lambda_{\Psi_B}\left(\mathcal{B}_x(\mathbf{o})|r_o^A\right) = \mathcal{G}(x,\lambda_B,R_{pz},r_o^A). \tag{58}$$

Corresponding conditional density function is given as

$$\lambda_{\Psi_B}(x|r_o^A) = \frac{1}{2\pi x}\frac{\mathrm{d}\Lambda_{\Psi_B}\left(\mathcal{B}_x(\mathbf{o})|r_o^A\right)}{\mathrm{d}x} = \mathcal{E}(x,\lambda_B,R_{pz},r_o^A), \tag{59}$$

where $\mathcal{E}$ is defined in Lemma 1. In the next step, to account for the rest of the PZs, independent thinning of the points in Ψ_B is performed with retention probability $\exp(-\pi\lambda_A R_{pz}^2)$ beyond the tagged OpA BS, which is at a distance r_o^A from the typical user. ∎

B. DISTRIBUTION OF DISTANCE TO THE NEAREST ACTIVE OpB BS

Conditioned on distance R_o^A, we are interested in the statistical characterization of the distance between the typical user and the nearest interfering OpB BS. In Fig. 2a, this distance is denoted by d_o^B, which is a realization of the random variable D_o^B. However, obtaining the distribution of D_o^B is not straightforward due to the following reasons:

1) the OpB BSs form a PHP process whose contact distribution is not known, and
2) due to contention based channel access, the nearest OpB BS in the PHP Φ_B to the typical user may not be the nearest active interfering BS.

To derive the distance distribution by exactly considering both the things mentioned above is left as a promising direction for future work. Instead, in the following Lemma, we derive an approximate distance distribution leveraging the conditional density function of Φ_B (in Lemma 15) and following the result presented in [25]. Note that, in contrast to our scenario, in [25] the locations of the contending BSs follow a homogeneous PPP.

Lemma 16: Conditioned on the serving distance R_o^A *between the typical user and the tagged OpA BS, the* PDF *of the distance* D_o^B *between the typical user and the nearest*

active OpB BS is given as

$$f_{D_o^B}(d_o^B|r_o^A) = 2\pi\tilde{\lambda}_{\Psi_B}(d_o^B|r_o^A)\eta(d_o^B|r_o^A)d_o^B \times \exp\left(-2\pi\int_{y=0}^{d_o^B}\tilde{\lambda}_{\Psi_B}(y|r_o^A)\eta(y|r_o^A)y\mathrm{d}y\right), \tag{60}$$

where $\tilde{\lambda}_{\Psi_B}(y|r_o^A)$ *is defined in Lemma 15,* $\eta(y|r_o^A)$ *is the probability that a point located at a distance y from the typical user wins contention, which is given as*

$$\eta(y|r_o^A) = \frac{1-\exp(-f_5(y,r_o^A))}{f_5(y,r_o^A)}, \tag{61}$$

and

$$f_5(y,r_o^A) = \int_{z=y}^{\infty}\int_{\theta=0}^{2\pi}\tilde{\lambda}_{\Psi_B}(z|r_o^A) \times \exp\left(\frac{-\tau_{cs}l(\sqrt{z^2+y^2-2zy\cos(\theta)})}{P_B}\right)\mathrm{d}\theta z\mathrm{d}z. \tag{62}$$

Proof: Please refer to Appendix H. ■

Although an approximation, above distance distribution is valid for a useful range of system parameters. In Fig. 10b, the theoretical CDF of D_o^B is compared with simulation results. The theoretical expression for $F_{D_o^B}(d_o^B)$ is given as

$$F_{D_o^B}(d_o^B) = \int_{r_o^A=0}^{\infty}\int_{z=0}^{d_o^B} f_{D_o^B}(z|r_o^A)f_{R_o^A}(r_o^A)\,\mathrm{d}z\,\mathrm{d}r_o^A. \tag{63}$$

C. THE DENSITY OF INTERFERING OpA BSs

In order to get the LT of the aggregate interference from OpA BSs, we need to take into account the distance to the nearest active OpB BS. In the following Lemma, we derive the density function for the interfering OpA BSs conditioned on R_o^A and D_o^B.

Lemma 17: Conditioned on the distances R_o^A *and* D_o^B*, the piece-wise density function of* Ψ_A *is given as*

$$\lambda_{\Psi_A}(x|r_o^A,d_o^B) = \frac{1}{2\pi x}\frac{\mathrm{d}\Lambda_{\Psi_A}\left(\mathcal{B}_x(\mathbf{o})|r_o^A,d_o^B\right)}{\mathrm{d}x}, \tag{64}$$

where $\Lambda_{\Psi_A}\left(\mathcal{B}_x(\mathbf{o})|r_o^A,d_o^B\right) = \mathcal{H}(x,d_o^B,r_o^A,R_{pz})$ *is the conditional intensity measure of the PPP* Ψ_A *and* $\mathcal{H}$ *is given by* (42) *with* λ_B *replaced by* λ_A.

Proof: The proof of this Lemma can be done on the similar lines as that of Lemma 12, and is hence skipped. ■

Using the conditional density functions of OpA and OpB BSs, and the distance to the nearest active interfering OpB BS, we present the coverage probability of a typical user served by OpA BS in the following proposition.

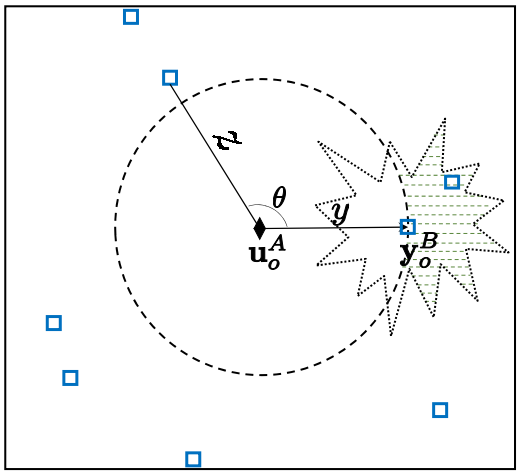

(a)

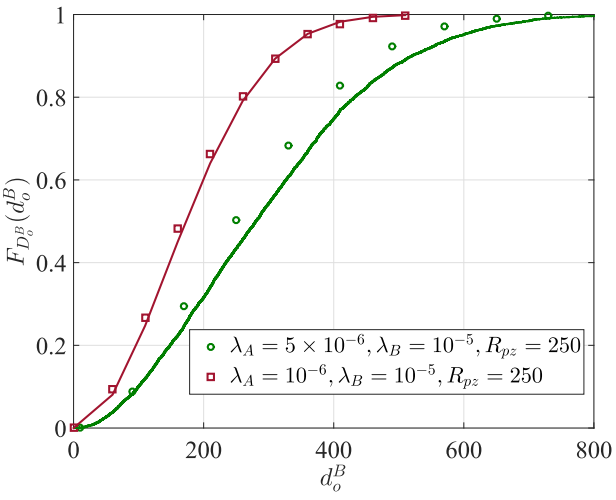

(b)

FIGURE 10. **(a) An illustration for Lemma 16. The dotted region represents the hypothetical contention domain of the OpB BS at $\mathbf{y}_o^B$. The contention domain shape is illustrated as irregular due to channel fading. (b) CDF of the distance between the nearest active OpB interferer and the typical user. $R_{pz} = 250$ m, $\tau_{cs} = -80$ dBm/10 MHz. Solid lines and markers represent the simulation and theoretical results, respectively.**

Proposition 2: The SIR *coverage probability for a typical OpA user at the origin is given as* $\mathtt{P}_{\mathtt{C}}^{(\mathtt{A})}(T) =$

$$\int_{r_o^A=0}^{\infty}\int_{d_o^B=0}^{\infty}\mathcal{L}_{I_{agg}^A}\left(\frac{Tl(r_o^A)}{P_A}\middle|r_o^A,d_o^B\right)f_{D_o^B}(d_o^B|r_o^A)\mathrm{d}d_o^B f_{R_o^A}(r_o^A)\mathrm{d}r_o^A, \tag{65}$$

where the PDFs $f_{R_o^A}(r_o^A)$ *and* $f_{D_o^B}(d_o^B|r_o^A)$ *are given by* (3) *and* (60)*, respectively, and the conditional* LT *of interference at the typical user is given as* $\mathcal{L}_{I_{agg}^A}\left(s|r_o^A,d_o^B\right) =$

$$\mathcal{L}_{I_{agg}^{AA}}\left(s|r_o^A,d_o^B\right)\mathcal{L}_{I_{agg}^{AB}}\left(s|r_o^A,d_o^B\right). \tag{66}$$

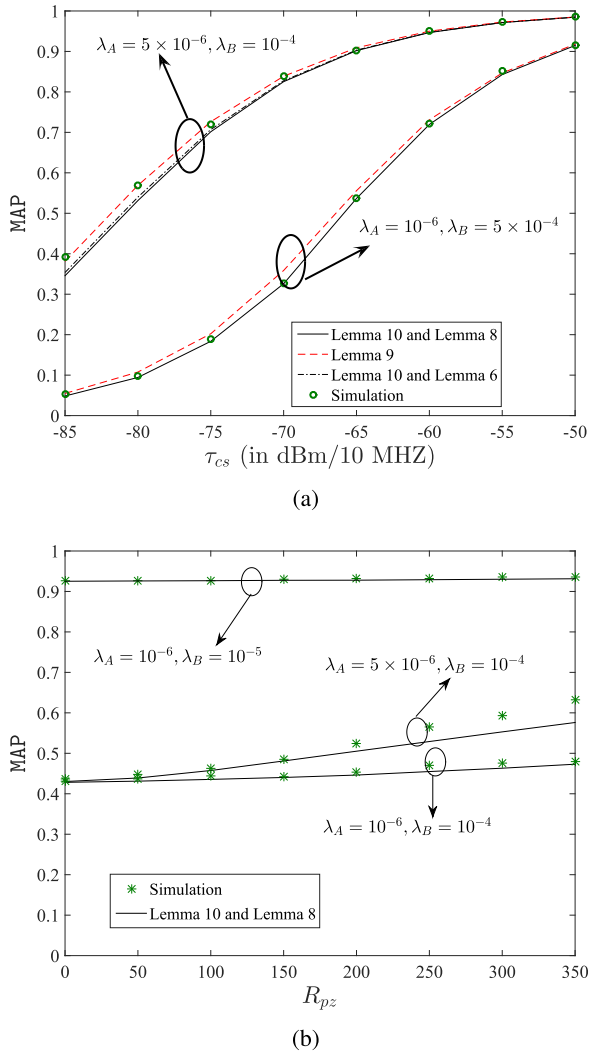

FIGURE 11. MAP of the tagged BS. (a) $R_{pz} = 250$ m. (b) $\tau_{cs} = -80$ dbm/10 MHz.

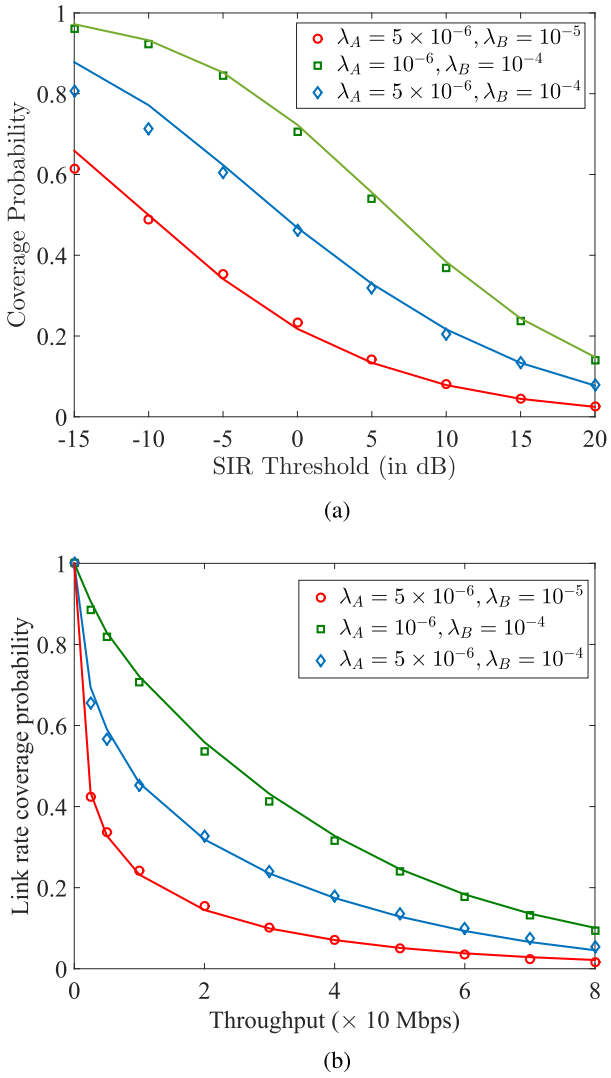

FIGURE 12. Markers represent simulation results and solid lines represent the theoretical results obtained from Proposition 1. $R_{pz} = 250$ m, $\tau_{cs} = -80$ dBm/10 MHz, $P_A = P_B = 30$ dBm/10 Mhz. (a) SIR coverage probability for the typical OpB user. (b) Link rate coverage probability for the typical OpB user.

In the above equation $\mathcal{L}_{I_{agg}^{AA}}\left(s|r_o^A, d_o^B\right) =$

$$\exp\left(-2\pi \int_{x=r_o^A}^{\infty} \frac{\lambda_{\Psi_A}(x|r_o^A, d_o^B)}{l(x)(sP_A)^{-1}+1} x \mathrm{d}x\right), \tag{67}$$

where $\lambda_{\Psi_A}(x|r_o^A, d_o^B)$ *is given in* (64). *Further,*

$$\mathcal{L}_{I_{agg}^{AB}}(s|r_o^A, d_o^B) = \frac{1}{1+\frac{sP_B}{l(d_o^B)}} \times \exp\left(-\int_{x=d_o^B}^{\infty} \int_{\theta=0}^{2\pi} \frac{\tilde{\lambda}_{\Psi_B}(x|r_o^A) M(\mathbf{x}(x,\theta)|d_o^B)}{l(x)(sP_B)^{-1}+1} \mathrm{d}\theta x \mathrm{d}x\right), \tag{68}$$

where $\tilde{\lambda}_{\Psi_B}(x|r_o^A)$ *is given in* (57). *The expression for* $M(\mathbf{x}(x,\theta)|d_o^B)$ *is provided in Lemma 13.*

Proof: This Proposition can be proved on similar line with Lemma 14 and Proposition 1. ■

VI. RESULTS AND DISCUSSION

In this section, the approximations made in the theoretical results are validated by simulations. Further, the performance analysis of both OpA and OpB network is also presented in terms of metrics discussed in the system model. The path loss model given in (7) is used for the system evaluation. Other system parameters are specified at appropriate places.

A. PERFORMANCE ANALYSIS OF OpB NETWORK

1) MAP OF THE TAGGED OpB BS

The effect of carrier sense threshold and protection zone radius on the MAP of the tagged OpB BS is presented in Figs. 11a and 11b. Note that to evaluate the lower bound of MAP presented in Lemma 10, the PDF of the contact distance of PHP is necessary. However, as mentioned in the system model, the contact distance distribution of PHP is an

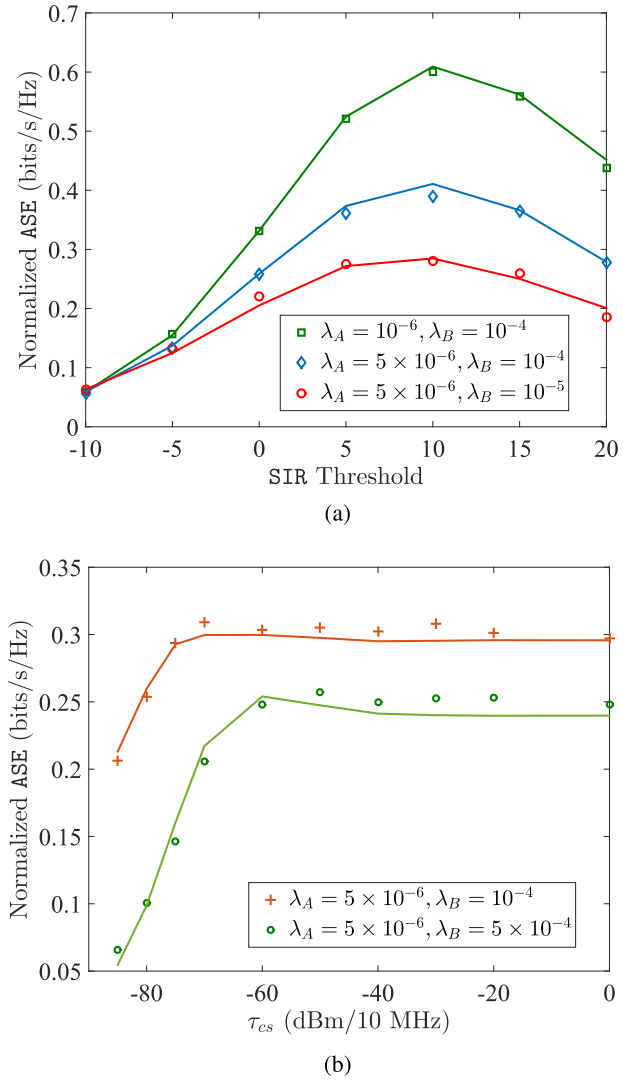

FIGURE 13. (a) Normalized ASE for different target SIR thresholds. $\tau_{cs} = -80$ dBm/10 MHz, $R_{pz} = 250$ m. (b) Normalized ASE for different carrier sense thresholds. Target SIR threshold is 0 dB, $R_{pz} = 250$ m. Lines and markers represent theoretical and simulation results, respectively. The MAP of the tagged BS is evaluated using Lemma 9.

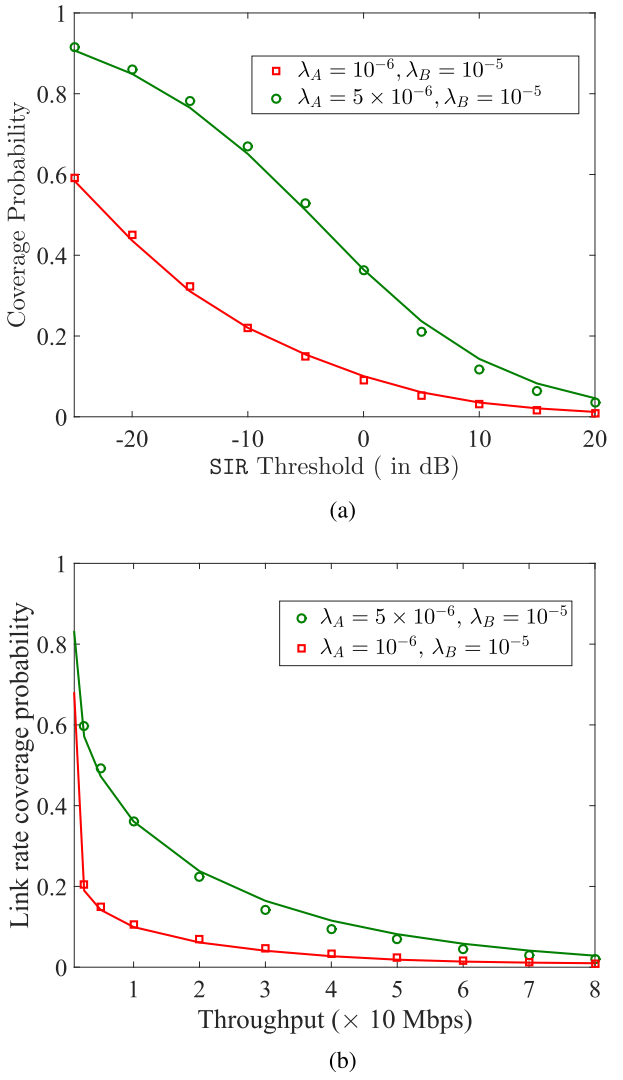

FIGURE 14. Markers represent simulation results and solid lines represent the theoretical results obtained from Proposition 2. $R_{pz} = 250$ m, $\tau_{cs} = -80$ dBm/10 MHz, $P_A = P_B = 30$ dBm/10 Mhz. (a) SIR coverage probability for the typical OpA user. (b) Link rate Coverage for a typical OpA user.

open problem, and for a given set of system parameters it is approximated as Weibull distribution. Hence, the results presented in Figs. 11a and 11b are not lower bounds in a true sense. However, as evident from the figures, the MAP evaluated using Lemma 10 and the approximated Weibull distribution acts as a tight bound with respect to different system parameters. In this case, the lower bound on the distribution of $R_{o,AB}$ presented in Lemma 8 is used. Further, the approximate result for MAP obtained from Lemma 9 matches closely with simulations. In Fig 11a, in accordance with intuition, as τ_{cs} increases, the MAP also increases since lesser number of BSs lie in the contention domain of the tagged BS. In addition, MAP of the tagged OpB BS for varying protection zone radii R_{pz} is presented in Fig. 11b. The effect of R_{pz} on MAP is less prominent compared to the carrier sense threshold, especially for lower density of OpA BSs. Further, from Fig. 11b, we observe that as λ_B increases, MAP reduces since more BSs contend for the channel. On the other hand, by increasing λ_A, the average number of OpB BSs decreases in the network, which improves the MAP of the tagged OpB BS.

2) COVERAGE PROBABILITY FOR A TYPICAL OpB USER

The SIR and the link rate coverage probabilities for a typical OpB user are presented in Figs. 12a and 12b. A close match between simulation and theoretical results is observed. Further, in both the cases, the coverage probability decreases with increasing λ_A. This can be justified by the fact that by increasing λ_A more interference is introduced into the network by the OpA BSs. Further, the serving distance between the typical user and the tagged OpB BS gets larger as the average number of OpB BSs reduces. On the other hand, increasing λ_B results in coverage probability improvement as the distance between

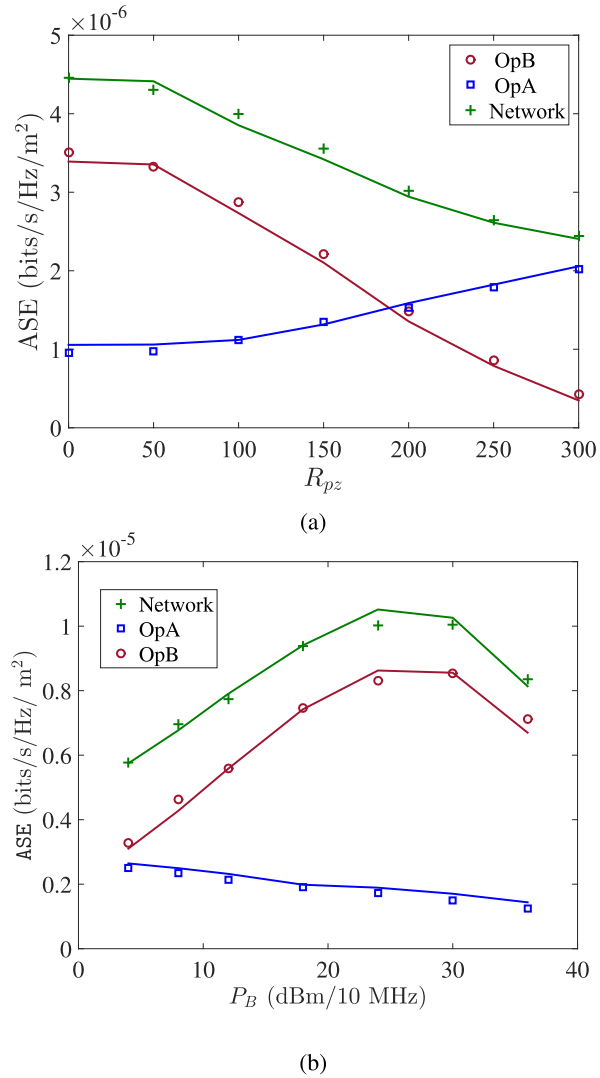

FIGURE 15. (a) Effect of R_{pz} on ASE. $T = 0$ dB, $P_A = P_B = 30$ dBm/10 MHz, $\tau_{cs} = -80$ dBm/10 MHz, $\lambda_A = 5 \times 10^{-6}$, $\lambda_B = 10^{-5}$. The MAP of the OpB tagged BS is evaluated using Lemmas 10 and 8. (b) Effect of P_B on ASE. $T = 0$ dB, $P_A = 36$ dBm/10 MHz, $\tau_{cs} = -80$ dBm/10 MHz, $\lambda_A = 5 \times 10^{-6}$, $\lambda_B = 10^{-4}$. The MAP of the OpB tagged BS is evaluated using Lemma 9.

the typical user and the tagged BS reduces, which improves the desired signal power.

3) NORMALIZED ASE FOR OpB NETWORK

The effect of different system parameters on normalized ASE of the OpB is presented in Figs. 13a and 13b. The ASE is normalized w.r.t. $\hat{\lambda}_B$. From Fig. 13a, we observe that by increasing λ_B or reducing λ_A, the normalized ASE improves. From Fig. 13b, it is clear that the impact of τ_{cs} on ASE is negligible beyond a certain threshold. The reason behind this behavior can be explained by the fact that by increasing τ_{cs}, the MAP of interfering BSs becomes unity, and the average interference contribution from the OpB BSs saturates. Hence, the overall coverage probability does not change with τ_{cs}.

B. PERFORMANCE ANALYSIS OF OpA NETWORK

The SIR and the link rate coverage probabilities of the typical OpA user are presented in Figs. 14a and 14b. A close match between the simulation and theoretical results is observed. As expected, by increasing λ_A, the coverage probability improves in both the cases.

C. NETWORK ASE ANALYSIS

The effect of PZ radius on the ASE of both the operators as well as the overall network ASE is presented in Fig. 15a. From the figure, it is clear that by increasing R_{pz}, overall ASE of the network goes down as a lesser number of OpB BSs are present in the network. The effect of OpB transmission power on the ASE is presented in Fig. 15b. In this figure, in order to evaluate coverage probability using Proposition 2, the joint PDF $f_{D_o^B, R_o^A}$ is obtained from Monte-Carlo simulations. From the figure, it is clear that OpB ASE is a concave function of P_B. Hence, proper optimization of P_B is necessary to maximize both network and OpB ASEs.

VII. CONCLUSION

In this work, we have presented the first comprehensive analysis of the co-existence between a licensed and unlicensed operator in the licensed band of the CBRS spectrum. Using tools from stochastic geometry, we have modeled the network as per the key recommendations from the FCC. Further, we have presented useful lower bound for the MAP of a serving unlicensed BS and fairly accurate coverage probability expressions for typical users of the licensed operator and unlicensed operator. The key technical novelty of this work lies in the way the correlation in the interference powers from licensed and unlicensed users is captured by accurately considering the local neighbourhood around the typical user. Using the derived expressions, we have studied the effect of PZ radius and transmission power of the unlicensed BSs on the area spectral efficiency of the network. One of the natural extensions of this work is network performance analysis considering an open access policy, and cooperation between the licensed and unlicensed operators. Further analysis is also possible in this direction by considering the presence of multiple licensed and unlicensed operators with and without cooperation. Other fundamental extensions include handling distance dependent power control by the unlicensed BSs, and consideration of directional CSMA-CA protocol [26] (which can be used to study mmWave systems).

APPENDIX

A. PROOF OF LEMMA 2

As discussed in Section III, in order to evaluate the MAP, we ignore the effect of all the PZs except the nearest one. In addition, due to the nearest neighbor connectivity, there are no OpB BSs in $\mathcal{B}_{r_o^B}(\mathbf{u}_o^B)$ (See Fig. 4b). Therefore, we consider the points in the set $\{x \in \Psi_B : x \notin \{\mathcal{B}_{R_{pz}}(\mathbf{y}_{oB}^A) \cup \mathcal{B}_{r_o^B}(\mathbf{u}_o^B)\}\}$. Using (9), the modified MAI of the tagged BS is

given as $\tilde{\mathcal{I}}_o^B =$

$$\prod_{\mathbf{x}_i^B \in \Psi_B \setminus \mathbf{x}_o^B} \mathbf{1}_{\mathbf{x}_i^B \notin \{\mathcal{B}_{R_{pz}}(\mathbf{y}_{oB}^A) \cup \mathcal{B}_{r_o^B}(\mathbf{u}_o^B)\}} \left(\mathbf{1}_{P_r(\mathbf{x}_o^B, \mathbf{x}_i^B) \leq \tau_{cs}} + \mathbf{1}_{P_r(\mathbf{x}_o^B, \mathbf{x}_i^B) > \tau_{cs}} \mathbf{1}_{t_{x_i}^B > t_{x_o}^B} \right). \quad (69)$$

Without loss of generality, we make the tagged BS as our reference point (i.e. origin) as shown in Fig. 4b. Let $\tilde{\Psi}_B = \{\mathbf{x} \in \Psi_B : \mathbf{x} \notin \mathcal{B}_{r_o^B}(\mathbf{u}_o^B)\}$. With application of Lemma 1, the density function of $\tilde{\Psi}_B$ is $\lambda_{\Psi_B}(x|r_o^B) = \mathcal{E}(x, \lambda_B, r_o^B, r_o^B)$. Now, conditioned on the distances R_o^B and $R_{o,AB} = \|\mathbf{y}_{oB}^A - \mathbf{x}_o^B\|$, and the back-off timer of the tagged BS $t_{x_o}^B = t$,

$$\begin{aligned}
&\mathbb{P}\left[\mathcal{I}_o^B = 1 \middle| t, r_{o,AB}, r_o^B\right] \\
&\overset{(a)}{\geq} \mathbb{P}\left[\tilde{\mathcal{I}}_o^B = 1 \middle| t, r_{o,AB}, r_o^B\right] = \mathbb{E}\left[\tilde{\mathcal{I}}_o^B \middle| t, r_{o,AB}, r_o^B\right] \\
&= \mathbb{E}\Bigg[\prod_{\mathbf{x}_i^B \in \tilde{\Psi}_B \setminus \{\mathcal{B}_{R_{pz}}(\mathbf{y}_{oB}^A) \cup \mathbf{x}_o^B\}} \mathbb{E}\Big[\mathbf{1}_{P_r(\mathbf{x}_o^B, \mathbf{x}_i^B) \leq \tau_{cs}} \\
&\quad + \mathbf{1}_{P_r(\mathbf{x}_o^B, \mathbf{x}_i^B) > \tau_{cs}} \mathbf{1}_{t < t_{x_i}^B} \Big] \Big| t, r_{o,AB}, r_o^B \Bigg] \\
&\overset{(b)}{=} \mathbb{E}\Bigg[\prod_{\mathbf{x}_i^B \in \tilde{\Psi} \setminus \{\mathcal{B}_{R_{pz}}(\mathbf{y}_{oB}^A) \cup \mathbf{x}_o^B\}} \left(1 - t \exp\left(-\frac{\tau_{cs} l(\|\mathbf{x}_i^B\|)}{P_B}\right)\right) \Bigg] \\
&\overset{(c)}{=} \exp\Bigg(- \int_{\mathbf{x} \in \mathbb{R}^2 \setminus \{\mathcal{B}_{R_{pz}}(\mathbf{y}_{oB}^A) \cup \mathbf{x}_o^B\}} t \lambda_{\Psi_B}(\|\mathbf{x}\| | r_o^B) e^{-\frac{\tau_{cs} l(\|\mathbf{x}\|)}{P_B}} \mathbf{x} d\mathbf{x} \Bigg) \\
&\overset{(d)}{=} \exp\Bigg(- t\Big(2\pi \int_0^\infty \lambda_{\Psi_B}(y|r_o^B) e^{\frac{-\tau_{cs} l(y)}{P_B}} y dy \\
&\quad - 2 \int_{r_{o,AB} - R_{pz}}^{r_{o,AB} + R_{pz}} \lambda_{\Psi_B}(y|r_o^B) e^{\frac{-\tau_{cs} l(y)}{P_B}} \varphi_{pz}(y|r_{o,AB}) y dy \Big) \Bigg), \quad (70)
\end{aligned}$$

where (a) follows from the fact that we are considering more number of points in $\tilde{\mathcal{I}}_o^B$ than in $\mathcal{I}_o^B$, (b) follows from the fact that small scale fading is exponentially distributed and $t_{x_i}^B$ is uniformly distributed between [0, 1], (c) follows from the application of the PGFL of the PPP, (d) follows from changing Cartesian co-ordinates to polar co-ordinates, and $\varphi_{pz}(y|r_{o,AB}) = \frac{r_{o,AB}^2 + y^2 - R_{pz}^2}{2 y r_{o,AB}}$. The expression for $f_1(\cdot)$ in Lemma 2 is obtained after deconditioning over $t_{x_o}^B$, which is uniformly distributed in [0, 1].

B. PROOF OF LEMMA 3

In this proof, we derive the conditional CDF of $R_{o,AB}$ for Event-2, i.e. the probability denoted by K_2 in (23). For notational simplicity we do not mention the condition $E_2(r_o^B) = \{N_{\Phi_B}(\mathcal{B}_{r_o^B}(\mathbf{u}_o^B)) = 0, N_{\Psi_B}(\mathcal{B}_{r_o^B}(\mathbf{u}_o^B)) = 0\}$ and implicitly consider it for all the expressions. Conditioned on R_o^B, the location of the nearest OpA BS from the typical user is constrained by the condition that it has to lie outside the circle $\mathcal{B}_{R_{pz}}(\mathbf{x}_o^B)$ (Refer to Fig. 6a). Now, at a distance r_o^A, the location of the nearest OpA BS lies on a ring. Hence, its location is uniformly distributed between the angles $[-\varphi_{AB}(r_o^A, r_o^B, R_{pz}), \varphi_{AB}(r_o^A, r_o^B, R_{pz})]$, where $\varphi_{AB}(r_o^A, r_o^B, R_{pz})$ is given by (29). Now the CDF of $R_{o,AB}$ conditioned on R_o^A, R_o^B, and Θ_A is given as

$$\begin{aligned}
&\mathbb{P}\left[R_{o,AB} \leq r_{o,AB} \middle| r_o^A, r_o^B, \theta_A\right] \\
&\overset{(a)}{=} \mathbb{P}\left[R_{o,AB} \leq r_{o,AB} \middle| N_{\Psi_A}\left(\mathcal{C}_1(\hat{r}_{o,AB})\right) = 0, r_o^A, r_o^B, \theta_A\right] \\
&\quad \times \mathbb{P}\left[N_{\Psi_A}\left(\mathcal{C}_1(\hat{r}_{o,AB})\right) = 0 \middle| r_o^A, r_o^B, \theta_A\right] \\
&\quad + \mathbb{P}\left[R_{o,AB} \leq r_{o,AB} \middle| N_{\Psi_A}\left(\mathcal{C}_1(\hat{r}_{o,AB})\right) \neq 0, r_o^A, r_o^B, \theta_A\right] \\
&\quad \times \mathbb{P}\left[N_{\Psi_A}\left(\mathcal{C}_1(\hat{r}_{o,AB})\right) \neq 0 \middle| r_o^A, r_o^B, \theta_A\right] \\
&\overset{(b)}{=} \mathbf{1}(\hat{r}_{o,AB} \leq r_{o,AB}) \exp(-\lambda_A |\mathcal{C}_1(\hat{r}_{o,AB})|) \\
&\quad + \mathbb{P}\left[\tilde{R}_{o,AB} \leq r_{o,AB} | r_o^A, r_o^B, \theta_A\right] \\
&\quad \times (1 - \exp(-\lambda_A |\mathcal{C}_1(\hat{r}_{o,AB})|)), \quad (71)
\end{aligned}$$

where (a) follows from the application of law of total probability, and (b) follows from (25) and the fact that number of points in $\mathcal{C}_1(\hat{r}_{o,AB})$ is Poisson distributed with mean $\lambda_A |\mathcal{C}_1(\hat{r}_{o,AB})|$. The second term in the summation is

$$\begin{aligned}
&\mathbb{P}\left[\tilde{R}_{o,AB} \leq r_{o,AB} | r_o^A, r_o^B, \theta_A\right] \\
&= \mathbb{P}\left[R_{o,AB} \leq r_{o,AB} | N_{\Psi_A}\left(\mathcal{C}_1(\hat{r}_{o,AB})\right) \neq 0, r_o^A, r_o^B, \theta_A\right] \\
&= \frac{\mathbb{P}\left[R_{o,AB} \leq r_{o,AB}, N_{\Psi_A}\left(\mathcal{C}_1(\hat{r}_{o,AB})\right) \neq 0 | r_o^A, r_o^B, \theta_A\right]}{\mathbb{P}\left[N_{\Psi_A}\left(\mathcal{C}_1(\hat{r}_{o,AB})\right) \neq 0 | r_o^A, r_o^B, \theta_A\right]} \\
&= \begin{cases} 1 & r_{o,AB} \geq \hat{r}_{o,AB} \\ \frac{1 - \exp(-\lambda_A |\mathcal{C}_1(r_{o,AB})|)}{1 - \exp(-\lambda_A |\mathcal{C}_1(\hat{r}_{o,AB})|)} & r_{o,AB} < \hat{r}_{o,AB}. \end{cases} \quad (72)
\end{aligned}$$

Substituting (72) in (71), we get

$$\begin{aligned}
&\mathbb{P}\left[R_{o,AB} \leq r_{o,AB} | r_o^A, r_o^B, \theta_A\right] \\
&= \mathbf{1}(\hat{r}_{o,AB} \leq r_{o,AB}) \exp(-\lambda_A |\mathcal{C}_1(\hat{r}_{o,AB})|) \\
&\quad + \mathbf{1}(\hat{r}_{o,AB} \leq r_{o,AB})(1 - \exp(-\lambda_A |\mathcal{C}_1(\hat{r}_{o,AB})|)) \\
&\quad + \mathbf{1}(\hat{r}_{o,AB} > r_{o,AB})(1 - \exp(-\lambda_A |\mathcal{C}_1(r_{o,AB})|)) \\
&= \mathbf{1}(\hat{r}_{o,AB} \leq r_{o,AB}) \\
&\quad + \mathbf{1}(\hat{r}_{o,AB} > r_{o,AB})(1 - \exp(-\lambda_A |\mathcal{C}_1(r_{o,AB})|)). \quad (73)
\end{aligned}$$

The final expression in the Lemma is obtained by deconditioning (73) w.r.t. conditional density function of Θ_A given in (28).

C. PROOF OF LEMMA 4

As per our discussion in Section III-A2 on Event-1 and Event-2, using the law of total probability, the distance distribution of R_o^A can be written as

$$\begin{aligned} F_{R_o^A}(r_o^A|r_o^B) &= \mathbb{P}\left[R_o^A \le r_o^A \middle| N_{\Phi_B}(\mathcal{B}_{r_o^B}(\mathbf{u}_o^B)) = 0, r_o^B\right] \\ &= \underbrace{\mathbb{P}\left[R_o^A \le r_o^A \middle| E_2(r_o^B), r_o^B\right]}_{T_1} \\ &\underbrace{\mathbb{P}\left[N_{\Psi_B}(\mathcal{B}_{r_o^B}(\mathbf{u}_o^B)) = 0 | N_{\Phi_B}(\mathcal{B}_{r_o^B}(\mathbf{u}_o^B)) = 0, r_o^B\right]}_{T_2} \\ &\quad + \underbrace{\mathbb{P}\left[R_o^A \le r_o^A \middle| E_1(r_o^B), r_o^B\right]}_{T_3} \\ &\underbrace{\mathbb{P}\left[N_{\Psi_B}(\mathcal{B}_{r_o^B}(\mathbf{u}_o^B)) \ne 0 | N_{\Phi_B}(\mathcal{B}_{r_o^B}(\mathbf{u}_o^B)) = 0, r_o^B\right]}_{T_4}, \end{aligned} \tag{74}$$

where the conditional CDF for Event-1 and Event-2 is denoted by T_3 and T_1, respectively.

Now for Event-2, the locations of OpA BSs follow a homogeneous PPP of density λ_A outside the circle $\mathcal{B}_{R_{pz}}(\mathbf{x}_o^B)$, which is equivalent to having a hole $\mathcal{B}_{R_{pz}}(\mathbf{x}_o^B)$ in Ψ_A. Therefore, with application of Lemma 1, the conditional CDF of R_o^A for Event-2 is

$$T_1 = 1 - \exp(-\mathcal{G}(r_o^A, \lambda_A, R_{pz}, r_o^B)). \tag{75}$$

On the other hand, T_3 corresponds to Event-1, where there is at least one OpA BS in $\mathcal{B}_{r_o^B+R_{pz}}(\mathbf{u}_o^B) \setminus \mathcal{B}_{R_{pz}}(\mathbf{x}_o^B)$ (Refer Fig. 5a). Further, to ensure that all the points of Ψ_B in $\mathcal{B}_{r_o^B}(\mathbf{u}_o^B)$ have been deleted, the conditional density of OpA BS in the $\mathcal{B}_{r_o^B+R_{pz}}(\mathbf{u}_o^B) \setminus \mathcal{B}_{R_{pz}}(\mathbf{x}_o^B)$ is likely to be higher than λ_A. Accurate characterization of this density requires exact consideration of number of PZs in the region and their relative overlaps, which is a difficult proposition. Hence, we consider the density of Ψ_A in $\mathcal{B}_{r_o^B+R_{pz}}(\mathbf{u}_o^B) \setminus \mathcal{B}_{R_{pz}}(\mathbf{x}_o^B)$ to be λ_A and obtain the CDF of T_3 given in (76) at the top of the next page. Note that since we are underestimating the density of Ψ_A, this conditional CDF is a lower bound on the actual CDF.

In order to obtain the probabilities given by T_3 and T_4, we observe that, we first need to determine $\mathbb{P}\left[N_{\Phi_B}(\mathcal{B}_{r_o^B}(\mathbf{u}_o^B)) = 0 | r_o^B\right]$, which is the complementary CDF of the contact distance of PHP, i.e. $\mathbb{P}\left[N_{\Phi_B}(\mathcal{B}_{r_o^B}(\mathbf{u}_o^B)) = 0 | r_o^B\right] = 1 - F_{R_o^B}(r_o^B)$. Now T_2 can be expressed as

$$\begin{aligned} &\mathbb{P}\left[N_{\Psi_B}(\mathcal{B}_{r_o^B}(\mathbf{u}_o^B)) = 0 | N_{\Phi_B}(\mathcal{B}_{r_o^B}(\mathbf{u}_o^B)) = 0, r_o^B\right] \\ &= \frac{\mathbb{P}\left[N_{\Psi_B}(\mathcal{B}_{r_o^B}(\mathbf{u}_o^B)) = 0 | r_o^B\right]}{\mathbb{P}\left[N_{\Phi_B}(\mathcal{B}_{r_o^B}(\mathbf{u}_o^B)) = 0 | r_o^B\right]} = \frac{\exp(-\pi\lambda_A(r_o^B)^2)}{1 - F_{R_o^B}(r_o^B)}. \end{aligned}$$

On the other hand, T_4 denotes the probability of the complementary event of $E_2(r_o^B)$ and its expression is given as

$$T_4 = 1 - T_2 = 1 - \frac{\exp(-\pi\lambda_A(r_o^B)^2)}{1 - F_{R_o^B}(r_o^B)}. \tag{77}$$

This completes the proof of the Lemma.

D. PROOF OF LEMMA 7

This Lemma can be proved on the similar lines as that of the proof of Lemma 4. First we approximate the CDF of R_o^A conditioned on Event-1, i.e. $F_{R_o^A}(r_o^A|r_o^B, E_1(r_o^B))$ presented in (74). As discussed earlier, conditioned on Event-1, the average number of OpA BSs in $\mathcal{B}_{r_o^B+R_{pz}}(\mathbf{u}_o^B) \setminus \mathcal{B}_{R_{pz}}(\mathbf{x}_o^B)$ is likely to be larger than $\lambda_A\pi\left((r_o^B + R_{pz})^2 - R_{pz}^2\right)$. While more rigorous approach can be used to obtain an accurate approximation for the above conditional CDF, we resort to a heuristic method to provide a simpler approximate expression for $F_{R_o^A}(r_o^A|r_o^B, E_1(r_o^B))$. First, we ignore the presence of the exclusion zone around the tagged BS. However, note that when $r_o^B < R_{pz}$, there will not be any OpA BSs in $\mathcal{B}_{R_{pz}-r_o^B}(\mathbf{u}_o^B)$. We take this into account to obtain the approximate expression. An illustration of the above scenario is presented in Fig. 5a, where the dotted red circle represents $\mathcal{B}_{R_{pz}-r_o^B}(\mathbf{u}_o^B)$. Second, for relatively larger values of $r_o^B (> R_{pz}/2)$, the number of OpA BSs in $\mathcal{B}_{r_o^B}(\mathbf{u}_o^B)$ is likely to be non-zero. Hence, we approximate that there is at least one OpA BS in $\mathcal{B}_{r_o^B}(\mathbf{u}_o^B) \setminus \mathcal{B}_{\max(R_{pz}-r_o^B,0)}(\mathbf{u}_o^B)$. Now, depending on the relative distances of r_o^B and R_{pz}, we get the expression presented in (35). The expression for $F_{R_o^A}(r_o^A|r_o^B, E_2(r_o^B))$ is the same the one given in (75).

Now our objective is to obtain approximate expressions for T_2 and T_4 in (74). The complementary CDF of R_o^B can be expressed as

$$\begin{aligned} &\mathbb{P}\left[N_{\Phi_B}(\mathcal{B}_{r_o^B}(\mathbf{u}_o^B)) = 0 | r_o^B\right] \\ &= \sum_{n=0}^{\infty} \mathbb{P}\left[N_{\Phi_B}(\mathcal{B}_{r_o^B}(\mathbf{u}_o^B)) = 0 | N_{\Psi_B}(\mathcal{B}_{r_o^B}(\mathbf{u}_o^B)) = n, r_o^B\right] \mathrm{Poi}(n) \\ &= \exp(-\pi\lambda_B(r_o^B)^2) \\ &\quad + \sum_{n=1}^{\infty} \mathbb{P}\left[N_{\Phi_B}(\mathcal{B}_{r_o^B}(\mathbf{u}_o^B)) = 0 | N_{\Psi_B}(\mathcal{B}_{r_o^B}(\mathbf{u}_o^B)) = n, r_o^B\right] \mathrm{Poi}(n), \end{aligned} \tag{78}$$

where

$$\mathrm{Poi}(n) = \exp(-\pi\lambda_B(r_o^B)^2)\frac{(\pi\lambda_B(r_o^B)^2)^n}{n!}. \tag{79}$$

In (77), presented in Appendix C, if we use the approximate CDF of R_o^B given in (5), then T_4 can be negative with non-zero probability. This is justified by the fact that the approximate expression cannot be decomposed into the total probability expression presented in (78). In order to avoid this situation, we approximate the complementary CDF

$$T_3 = \mathbb{P}\left[R_o^A \le r_o^A \middle| E_1(r_o^B), r_o^B\right] = \begin{cases} 0 & r_o^A \le R_{pz} - r_o^B \\ \frac{1-\exp(-\lambda_A|\mathcal{C}_2(r_o^A, r_o^B, R_{pz})|)}{1-\exp(-\lambda_A|\mathcal{C}_2(r_o^B+R_{pz}, r_o^B, R_{pz})|)} & R_{pz} - r_o^B < r_o^A \le R_{pz} + r_o^B, \end{cases} \tag{76}$$

where $\mathcal{C}_2(r_o^A, r_o^B, R_{pz}) = \mathcal{B}_{r_o^A}(\mathbf{u}_o^B) \setminus \{\mathcal{B}_{r_o^A}(\mathbf{u}_o^B) \cap \mathcal{B}_{R_{pz}}(\mathbf{x}_o^B)\}$.

of R_o^B as

$$\begin{aligned} 1 - F_{R_o^B}(r_o^B) &= \mathbb{P}\left[N_{\Phi_B}(\mathcal{B}_{r_o^B}(\mathbf{u}_o^B)) = 0 | r_o^B\right] \\ &\approx \exp(-\pi\lambda_B (r_o^B)^2) \\ &\quad + \sum_{n=1}^{\infty} \left(1 - \exp(-\pi\lambda_A R_{pz}^2)\right)^n \mathrm{Poi}(n) \\ &= \exp(-\pi\lambda_B \exp(-\pi\lambda_A R_{pz}^2)(r_o^B)^2), \end{aligned} \tag{80}$$

where the second step follows from the fact that there exists at least one PAL BS within R_{pz} of each of the n points so that all the n points have been deleted. Since the relative overlaps among protection zones are ignored, the above expression is an approximation. The third step follows after some algebraic manipulation. Now, the complementary CDF of R_o^B in the Lemma can be approximated by the expression presented in (80).

E. PROOF OF LEMMA 8

Note that if we take into account only Event-2, then we are underestimating the density of OpA BSs in the vicinity of the tagged OpB BS. Therefore, the actual distance is stochastically dominated (first order) by the distance obtained considering only Event-2. Using this fact, we derive the lower bound on the CDF that is presented next. From (22), using the law of total probability we write $F_{R_{o,AB}}(r_{o,AB}|r_o^B) =$

$$\begin{aligned} &\mathbb{P}\left[R_{o,AB} \le r_{o,AB} | r_o^B, N_{\Phi_B}(\mathcal{B}_{r_o^B}(\mathbf{u}_o^B)) = 0\right] \\ &\quad = \mathbb{P}\left[R_{o,AB} \le r_{o,AB} | r_o^B, E_1(r_o^B)\right] \\ &\mathbb{P}\left[N_{\Psi_B}(\mathcal{B}_{r_o^B}(\mathbf{u}_o^B)) \ne 0 | N_{\Phi_B}(\mathcal{B}_{r_o^B}(\mathbf{u}_o^B)) = 0, r_o^B\right] \\ &\qquad + \mathbb{P}\left[R_{o,AB} \le r_{o,AB} | r_o^B, E_2(r_o^B)\right] \\ &\mathbb{P}\left[N_{\Psi_B}(\mathcal{B}_{r_o^B}(\mathbf{u}_o^B)) = 0 | N_{\Phi_B}(\mathcal{B}_{r_o^B}(\mathbf{u}_o^B)) = 0, r_o^B\right] \\ &\quad \overset{(a)}{\ge} \mathbb{P}\left[R_{o,AB} \le r_{o,AB} | r_o^B, E_2(r_o^B)\right] \\ &\left(\mathbb{P}\left[N_{\Psi_B}(\mathcal{B}_{r_o^B}(\mathbf{u}_o^B)) \ne 0 | N_{\Phi_B}(\mathcal{B}_{r_o^B}(\mathbf{u}_o^B)) = 0, r_o^B\right]\right. \\ &\qquad \left. + \mathbb{P}\left[N_{\Psi_B}(\mathcal{B}_{r_o^B}(\mathbf{u}_o^B)) = 0 | N_{\Phi_B}(\mathcal{B}_{r_o^B}(\mathbf{u}_o^B)) = 0, r_o^B\right]\right) \\ &\quad \overset{(b)}{=} \mathbb{P}\left[R_{o,AB} \le r_{o,AB} | r_o^B, E_2(r_o^B)\right], \end{aligned}$$

where (a) follows since we are considering only Event-2 and

$$\begin{aligned} &\mathbb{P}\left[R_{o,AB} \le r_{o,AB} | r_o^B, E_2(r_o^B)\right] \\ &\quad \le \mathbb{P}\left[R_{o,AB} \le r_{o,AB} | r_o^B, E_1(r_o^B)\right]. \end{aligned} \tag{81}$$

In order to evaluate the probability in (b), note that the OpA BS forms a homogeneous PPP of density λ_A beyond $\mathcal{B}_{R_{pz}}(\mathbf{x}_o^B)$. Further, as discussed in Section III-A2, for Event-2, $R_{o,AB}$ is independent of R_o^B. Hence, using [23, Lemma 4], we write

$$F_{R_{o,AB}}(r_{o,AB}|r_o^B) \ge 1 - \exp\left(-\pi\lambda_A((r_{o,AB})^2 - R_{pz}^2)\right),$$

and the final expression in the Lemma follows from deconditioning w.r.t. R_o^B.

F. PROOF OF LEMMA 10

In order to prove this Lemma, we first need to show that deconditioning w.r.t. $R_{o,AB}$ using a lower bound on its CDF preserves the lower bound on the conditional MAP presented in Lemma 2. To arrive at this conclusion, consider the expression in step (d) in (70) presented in Appendix A. The lower bound on the MAP of the tagged BS conditioned on $R_{o,AB}$, R_o^B, $t_{x_o^B}$ is given as

$$\begin{aligned} &\mathbb{P}\left[\mathcal{I}_o^B | r_{o,AB}, r_o^B, t\right] \\ &\quad \ge \exp\Bigg(-t\Big(2\pi \int_0^{\infty} \lambda_{\Psi_B}(y|r_o^B) e^{\frac{-\tau_{cs} l(y)}{P_B}} y \mathrm{d}y \\ &\qquad - 2 \int_{r_{o,AB}-R_{pz}}^{r_{o,AB}+R_{pz}} \lambda_{\Psi_B}(y|r_o^B) e^{\frac{-\tau_{cs} l(y)}{P_B}} \varphi_{pz}(y|r_{o,AB}) y \mathrm{d}y\Big)\Bigg) \\ &\quad = \exp\left(-tf_1(r_{o,AB}, r_o^B)\right). \end{aligned}$$

Since $f_1(r_{o,AB}, r_o^B)$ is an increasing function w.r.t. $r_{o,AB}$, conditioned on R_o^B and $t_{x_o^B}$ we write

$$\begin{aligned} &\int_{r_{o,AB}=R_{pz}}^{\infty} e^{-tf_1(r_{o,AB}, r_o^B)} \mathrm{d}F_{R_{o,AB}}(r_{o,AB}|r_o^B) \\ &\quad \ge \int_{r_{o,AB}=R_{pz}}^{\infty} e^{-tf_1(r_{o,AB}, r_o^B)} \mathrm{d}F_{R_{o,AB}}^{\mathrm{LB},\mathtt{x}}(r_{o,AB}|r_o^B), \end{aligned} \tag{82}$$

where $F_{R_{o,AB}}^{\mathrm{LB},\mathtt{x}}(r_{o,AB}|r_o^B)$ denotes the lower bounds on the CDF of $R_{o,AB}$ presented in Lemmas 6 and 8. Now, de-conditioning

the above expressions w.r.t. $t_{x_o^B}$ and R_o^B, we get

$$\mathbb{P}\left[\mathcal{I}_o^B | r_{o,AB}, r_o^B, t\right] \geq \int_{r_o^B=0}^{\infty} \int_{t=0}^{1} \int_{r_{o,AB}=R_{pz}}^{\infty} e^{-tf_1(r_{o,AB}, r_o^B)} \times \mathrm{d}F_{R_{o,AB}}^{\mathrm{LB},\times}(r_{o,AB}|r_o^B) f_{R_o^B}(r_o^B)\mathrm{d}t\mathrm{d}r_o^B.$$

Changing the order of integration between $r_{o,AB}$ and t, and deconditioning w.r.t. $t_{x_o^B}$ we arrive at the result presented in the Lemma.

G. PROOF OF LEMMA 14

Since the density functions in Lemmas 11 and 12 are conditioned on the distances to the nearest OpA BS and the tagged OpB BS, the correlation in node locations is effectively captured by these conditional densities in the vicinity of the typical user. Hence, conditioned on R_o^A and R_o^B, we assume that these interference powers are independent of each other.

Now, the conditional LT of the aggregate interference can be expressed as the product of the conditional LTs of interference from OpA and OpB BSs. Following the similar approach as presented in [14], the LT of interference from the interfering OpB BSs conditioned on R_o^A, R_o^B, and $\mathcal{I}_o^B = 1$ is given as $\mathcal{L}_{I_{agg}^{BB}}(s|r_o^A, r_o^B, \mathcal{I}_o^B = 1) =$

$$\mathbb{E}\left[e^{-s\sum_{\mathbf{x}_j\in\Phi_B\setminus\mathbf{x}_o^B} \frac{P_B\mathcal{I}_j^B h(\mathbf{u}_o^B,\mathbf{x}_j)}{l(\|\mathbf{x}_j\|)}} \middle| r_o^A, r_o^B, \mathcal{I}_o^B = 1\right]$$
$$= \mathbb{E}\left[\prod_{\mathbf{x}_j\in\Phi_B\setminus\mathbf{x}_o^B} \mathbb{E}\left[e^{\frac{-s\mathcal{I}_j^B P_B h(\mathbf{u}_o^B,\mathbf{x}_j)}{l(\|\mathbf{x}_j\|)}}\right] \middle| r_o^A, r_o^B, \mathcal{I}_o^B = 1\right]$$
$$\overset{(a)}{=} \mathbb{E}\left[\prod_{\mathbf{x}_j\in\Phi_B\setminus\mathbf{x}_o^B} \frac{1}{1+\frac{s\mathcal{I}_j^B P_B}{l(\|\mathbf{x}_j\|)}} \middle| r_o^A, r_o^B, \mathcal{I}_o^B = 1\right]$$
$$\overset{(b)}{=} \exp\left(-\int_{x=r_o^B}^{\infty}\int_{\theta=0}^{2\pi} \frac{\tilde{\lambda}_{\Psi_B}(x|r_o^A, r_o^B)M(\mathbf{x}(x,\theta)|r_o^B)}{l(x)(sP_B)^{-1}+1}\mathrm{d}\theta x\mathrm{d}x\right), \quad (83)$$

where (a) follows from the moment generating function (MGF) of the exponential fading term $h(\mathbf{u}_o^B, \mathbf{x}_j)$, (b) follows from the application of the PGFL of PPP and the retention probability of a point in Φ_B derived in Lemma 13. Similarly, the conditional LT of interference from the OpA BSs is $\mathcal{L}_{I_{agg}^{BA}}(s|r_o^A, r_o^B) =$

$$\mathbb{E}\left[e^{\left(-s\frac{P_A h(\mathbf{u}_o^B,\mathbf{x}_o^A)}{l(\|\mathbf{x}_o^A\|)} - \sum_{\mathbf{y}_j\in\Psi_A\setminus\mathbf{x}_o^A} \frac{sP_A h(\mathbf{u}_o^B,\mathbf{y}_j)}{l(\|\mathbf{y}_j\|)}\right)}\right]$$
$$= \mathbb{E}_h\left[e^{\frac{-sP_A h(\mathbf{u}_o^B,\mathbf{x}_o^A)}{l(r_o^A)}}\right]\mathbb{E}_{\Psi_A}\left[\prod_{\mathbf{y}_j\in\Psi_A\setminus\mathbf{x}_o^A}\mathbb{E}_h\left[e^{\left(-\frac{sP_A h(\mathbf{u}_o^B,\mathbf{y}_j)}{l(\|\mathbf{y}_j\|)}\right)}\right]\right]$$
$$= \frac{1}{1+\frac{sP_A}{l(r_o^A)}}\exp\left(-2\pi\int_{y=r_o^A}^{\infty}\frac{\mathcal{E}(y,\lambda_A,R_{pz},r_o^B)}{l(y)(sP_A)^{-1}+1}y\mathrm{d}y\right),$$

where the last step follows from the application of the PGFL of PPP, and the conditional density of Ψ_A is presented in (40).

H. PROOF OF LEMMA 16

As illustrated in Fig. 10a, consider an OpB BS located at $\mathbf{y}_o^B$ and let $y = \|\mathbf{y}_o^B\|$. Note that Fig. 10a presents a representative diagram for Φ_B that has been approximated as a non-homogeneous PPP using Lemma 15. Hence, we have already captured the effect of all the PZs in the network. If we do not take into account the contention process among the BSs in Φ_B, then the CDF of the distance between the typical user and the nearest interfering BS conditioned on R_o^A is given as

$$F_{D_o^B}(d_o^B|r_o^A) = 1 - \mathbb{P}\left[N_{\Phi_B}(\mathcal{B}_{d_o^B}(\mathbf{u}_o^A)|r_o^A) = 0\right]$$
$$= 1 - \exp\left(-2\pi\int_{y=0}^{d_o^B}\tilde{\lambda}_{\Psi_B}(y|r_o^A)y\mathrm{d}y\right), \quad (84)$$

which follows from the nearest neighbor distribution of a non-homogeneous PPP. One way of interpreting this result is that all the BSs in Φ_B have a retention probability 1. On the other hand, if contention process is considered among the BSs in Φ_B, then all the BSs are not going to be active (retained), which depends on the MAP of a BS in Φ_B. Hence, the nearest BS in Φ_B may not be the first active interfering BS. In order to obtain the distance distribution to the nearest active BS, we follow the similar assumption as presented in [25, Sec. IV]. As per the assumption, the contention domain of a BS located at a distance y from the origin (in our case the typical OpA user) lies beyond $\mathcal{B}_y(\mathbf{u}_o^A)$. Hence, the medium access indicator for the BS at $\mathbf{y}_o^B$ is given as $\mathcal{I}_{\mathbf{y}_o}^B =$

$$\prod_{\mathbf{x}_j^B\in\Phi_B\setminus\mathcal{B}_y(\mathbf{u}_o^A)}\left(\mathbf{1}_{P_r(\mathbf{y}_o^B,\mathbf{x}_j^B)\leq\tau_{cs}} + \mathbf{1}_{P_r(\mathbf{y}_o^B,\mathbf{x}_j^B)>\tau_{cs}}\mathbf{1}_{t_{x_j}^B > t_{y_o}^B}\right). \quad (85)$$

Now using the similar steps as presented in Appendix A, the MAP of a BS at a distance y from the origin is given as

$$\eta(y|r_o^A) = \mathbb{E}\left[\mathcal{I}_{\mathbf{y}_o}^B = 1\right] = \frac{1-\exp(-f_5(y,r_o^A))}{f_5(y,r_o^A)}, \quad (86)$$

where $f_5(y, r_o^A)$ is presented in (62). Above MAP can be interpreted as the retention probability of the point at $\mathbf{y}_o^B \in \Phi_B$ as an active interferer. Using the above retention probability, we assume that the active BSs in Φ_B form a non-homogeneous PPP of density $\tilde{\lambda}_{\Psi_B}(y|r_o^A)\eta(y|r_o^A)$. Hence, the CDF of distance to the nearest active OpB interfering BS conditioned on r_o^A is given as

$$F_{D_o^B}(d_o^B|r_o^A) = 1 - \exp\left(-2\pi\int_{y=0}^{d_o^B}\tilde{\lambda}_{\Psi_B}(y|r_o^A)\eta(y|r_o^A)y\mathrm{d}y\right). \quad (87)$$

The conditional PDF in the Lemma is obtained by taking the derivative of the above CDF w.r.t. d_o^B.

Acknowledgment

This work was presented in part at the IEEE WCNC workshop [1].

REFERENCES

[1] P. Parida, H. S. Dhillon, and P. Nuggehalli, "Stochastic geometry perspective of unlicensed operator in a CBRS system," in *Proc. IEEE Wireless Commun. Netw. Conf. Workshops (WCNC Workshops)*, San Francisco, CA, USA, Mar. 2017.

[2] "Cisco visual networking index: Global mobile data traffic forecast update, 2015–2020," Cisco, San Jose, CA, USA, Tech. Rep., 2015.

[3] "Report and order and second further notice of proposed rule making," Federal Commun. Commission, Washington, DC, USA, Tech. Rep. GN Docket No. 12-354, Apr. 2016.

[4] J. H. Reed *et al.*, "On the co-existence of TD-LTE and radar over 3.5 GHz band: An experimental study," *IEEE Wireless Commun. Lett.*, vol. 5, no. 4, pp. 368–371, Aug. 2016.

[5] S. Bhattarai, A. Ullah, J.-M. J. Park, J. H. Reed, D. Gurney, and B. Gao, "Defining incumbent protection zones on the fly: Dynamic boundaries for spectrum sharing," in *Proc. IEEE Int. Symp. Dyn. Spectr. Access Netw. (DySpan)*, Sep./Oct. 2015, pp. 251–262.

[6] C. W. Kim, J. Ryoo, and M. M. Buddhikot, "Design and implementation of an end-to-end architecture for 3.5 GHz shared spectrum," in *Proc. IEEE Int. Symp. Dyn. Spectr. Access Netw. (DySpan)*, Sep./Oct. 2015, pp. 23–34.

[7] J. G. Andrews, F. Baccelli, and R. K. Ganti, "A tractable approach to coverage and rate in cellular networks," *IEEE Trans. Commun.*, vol. 59, no. 11, pp. 3122–3134, Nov. 2011.

[8] H. S. Dhillon, R. K. Ganti, F. Baccelli, and J. G. Andrews, "Modeling and analysis of K-tier downlink heterogeneous cellular networks," *IEEE J. Sel. Areas Commun.*, vol. 30, no. 3, pp. 550–560, Apr. 2012.

[9] H. Elsawy, E. Hossain, and M. Haenggi, "Stochastic geometry for modeling, analysis, and design of multi-tier and cognitive cellular wireless networks: A survey," *IEEE Commun. Surveys Tuts.*, vol. 15, no. 3, pp. 996–1019, 3rd Quart., 2013.

[10] M. Haenggi, *Stochastic Geometry for Wireless Networks*. Cambridge, U.K.: Cambridge Univ. Press, 2013.

[11] S. Mukherjee, *Analytical Modeling of Heterogeneous Cellular Networks: Geometry, Coverage, and Capacity*. Cambridge, U.K.: Cambridge Univ. Press, Jan. 2014.

[12] J. G. Andrews, A. K. Gupta, and H. S. Dhillon. (2016). "A primer on cellular network analysis using stochastic geometry." [Online]. Available: https://arxiv.org/abs/1604.03183

[13] H. ElSawy, A. Sultan-Salem, M.-S. Alouini, and M. Z. Win, "Modeling and analysis of cellular networks using stochastic geometry: A tutorial," *IEEE Commun. Surveys Tuts.*, vol. 19, no. 1, pp. 167–203, 1st Quart., 2017.

[14] H. Q. Nguyen, F. Baccelli, and D. Kofman, "A stochastic geometry analysis of dense IEEE 802.11 networks," in *Proc. IEEE Int. Conf. Comput. Commun.*, May 2007, pp. 1199–1207.

[15] G. Alfano, M. Garetto, and E. Leonardi, "New directions into the stochastic geometry analysis of dense CSMA networks," *IEEE Trans. Mobile Comput.*, vol. 13, no. 2, pp. 324–336, Feb. 2014.

[16] T. V. Nguyen and F. Baccelli, "A probabilistic model of carrier sensing based cognitive radio," in *Proc. IEEE Symp. New Frontiers Dyn. Spectr.*, Apr. 2010, pp. 1–12.

[17] N. T. Viet and F. Baccelli, "Stochastic modeling of carrier sensing based cognitive radio networks," in *Proc., Modeling Optim. Mobile, Ad Hoc Wireless Netw.*, May 2010, pp. 472–480.

[18] Y. Li, F. Baccelli, J. G. Andrews, T. D. Novlan, and J. C. Zhang, "Modeling and analyzing the coexistence of Wi-Fi and LTE in unlicensed spectrum," *IEEE Trans. Wireless Commun.*, vol. 15, no. 9, pp. 6310–6326, Sep. 2016.

[19] C.-H. Lee and M. Haenggi, "Interference and outage in Poisson cognitive networks," *IEEE Trans. Wireless Commun.*, vol. 11, no. 4, pp. 1392–1401, Apr. 2012.

[20] X. Song, C. Yin, D. Liu, and R. Zhang, "Spatial throughput characterization in cognitive radio networks with threshold-based opportunistic spectrum access," *IEEE J. Sel. Areas Commun.*, vol. 32, no. 11, pp. 2190–2204, Nov. 2014.

[21] U. Tefek and T. J. Lim, "Interference management through exclusion zones in two-tier cognitive networks," *IEEE Trans. Wireless Commun.*, vol. 15, no. 3, pp. 2292–2302, Mar. 2016.

[22] N. Deng, W. Zhou, and M. Haenggi, "Heterogeneous cellular network models with dependence," *IEEE J. Sel. Areas Commun.*, vol. 33, no. 10, pp. 2167–2181, Oct. 2015.

[23] Z. Yazdanshenasan, H. S. Dhillon, M. Afshang, and P. H. J. Chong, "Poisson hole process: Theory and applications to wireless networks," *IEEE Trans. Wireless Commun.*, vol. 15, no. 11, pp. 7531–7546, Nov. 2016.

[24] "Guidelines for Evaluation of Radio Interface Technologies for IMT-Advanced," document M.2135, ITU-R, 2009.

[25] A. Al-Hourani, R. J. Evans, and S. Kandeepan, "Nearest neighbor distance distribution in hard-core point processes," *IEEE Commun. Lett.*, vol. 20, no. 9, pp. 1872–1875, Sep. 2016.

[26] M. X. Gong, R. Stacey, D. Akhmetov, and S. Mao, "A directional CSMA/CA protocol for mmWave wireless PANs," in *Proc. IEEE Wireless Commun. Netw. Conf. (WCNC)*, Apr. 2010, pp. 1–6.

PRIYABRATA PARIDA (S'14) received the B.Tech. degree in electronics and communications engineering from the National Institute of Technology, Durgapur, India, in 2010, and the M.S. degree in telecommunications from the IIT Kharagpur, Kharagpur, India, in 2015. He is currently pursuing the Ph.D. degree at Virginia Tech, where his research interest includes modeling and analysis of fifth generation cellular networks using tools from stochastic geometry. His other research interests lie in the domain of MIMO and resource allocation in wireless systems. He has held an internship position at MediaTek Inc., San Jose, USA, during 2016.

HARPREET S. DHILLON (S'11–M'13) received the B.Tech. degree in electronics and communication engineering from IIT Guwahati, India, in 2008, the M.S. degree in electrical engineering from Virginia Tech, Blacksburg, VA, USA, in 2010, and the Ph.D. degree in electrical engineering from the University of Texas at Austin, Austin, TX, USA, in 2013. After a postdoctoral year at the University of Southern California, Los Angeles, CA, USA, he joined Virginia Tech in 2014, where he is currently an Assistant Professor of Electrical and Computer Engineering. He has held internships at Alcatel-Lucent Bell Labs in Crawford Hill, NJ, USA, Samsung Research America, Richardson, TX, USA, Qualcomm Inc., San Diego, CA, USA, and Cercom, Politecnico di Torino, Italy. His research interests include communication theory, stochastic geometry, geolocation, and wireless ad hoc and heterogeneous cellular networks.

Dr. Dhillon has been a co-author of five best paper award recipients, including the 2016 IEEE Communications Society (ComSoc) Heinrich Hertz Award, the 2015 IEEE ComSoc Young Author Best Paper Award, the 2014 IEEE ComSoc Leonard G. Abraham Prize, the 2014 European Wireless Best Student Paper Award, and the 2013 IEEE International Conference in Communications Best Paper Award in the Wireless Communications Symposium. He was also the recipient of the USC Viterbi Post-Doctoral Fellowship, the 2013 UT Austin Wireless Networking and Communications Group Leadership Award, the UT Austin Microelectronics and Computer Development Fellowship, and the 2008 Agilent Engineering and Technology Award. He is currently an Editor of the IEEE TRANSACTIONS ON WIRELESS COMMUNICATIONS, the IEEE TRANSACTIONS ON GREEN COMMUNICATIONS AND NETWORKING, and the IEEE WIRELESS COMMUNICATIONS LETTERS.

PAVAN NUGGEHALLI (S'98–M'03) received the B.Tech. degree in electronics and communication engineering from the Regional Engineering College at Kurukshetra, India, in 1996, the M.Sc. (Engg.) degree in electrical sciences from the Indian Institute of Science, Bangalore, in 1998, and the Ph.D. degree in electrical and computer engineering from the University of California at San Diego in 2003. He has worked in both academic and industrial settings. From 2003 to 2007, he was an Assistant Professor with the Indian Institute of Science and a Visiting Researcher from 2006 to 2007 with the University of California at San Diego. Since 2007, he has been employed at several companies, including Vanu, Beceem, Samsung, Broadcom, and MediaTek.

Dr. Nuggehalli is currently a Technical Manager with MediaTek in San Jose, California, where he represents MediaTek in 3GPP's RAN2 working group. He has authored over 30 papers in peer-reviewed journals and conferences and served on the technical program committees of several premier conferences. His research interests comprise modeling, analysis, and simulation of wireless protocols at the MAC, network, and transport layers.